이학박사 학위논문

Strong coupling between terahertz nano-slot antenna and metallic nano-objects

테라헤르츠 나노 슬롯 안테나와 금속 나노 물질 사이의 강한 상호 작용

2012 년 8 월

서울대학교 대학원

물리천문학부 물리학 전공

박 형 렬

Strong coupling between terahertz nano-slot antenna and metallic nano-objects

지도 교수 김 대 식

이 논문을 이학박사 학위논문으로 제출함

2012 년 8 월

서울대학교 대학원

물리천문학부 물리학 전공

박 형 렬

박형렬의 이학박사 학위논문을 인준함

2012 년 8 월

위 원 장 박 건 식 (인)

부위원장 김 대 식 (인)

위 원 전 헌 수 (인)

위 원 최 석 봉 (인)

위 원 신 종 화 (인)

Strong coupling between terahertz nano-slot antenna and metallic nano-objects

by

Hyeong-Ryeol Park

Supervised by

Prof. Dai-Sik Kim

A Dissertation Submitted to the Faculty of Seoul National University in Candidacy for the Degree of Doctor of Philosophy

August 2012

Department of Physics and Astronomy

Graduate School

Seoul National University

Abstract

Strong coupling between terahertz nano-slot antenna and metallic nano-objects

Hyeong-Ryeol Park

Department of Physics and Astronomy

The Graduate School

Seoul National University

Optical antennas have received much interest with the ability to generate resonantly enhanced local fields and to detect nanoparticles and biomolecules. Strong local fields could increase the scattering or the nonlinear emission from particles thereby enabling detection of subwavelength particles beyond the diffraction limit. Based on these attempts, we would transplant the concept of optical antennas into terahertz nano-slot antenna with hundreds micron length and nano-sized width, leading to new functionalities in terms of nanoscale control of terahertz electromagnetic wave. In this thesis, we will demonstrate strong coupling between nano-slot antenna and metallic nanoparticles with the volume much smaller than $\left(\frac{\lambda}{1{,}000}\right)^3$ in the terahertz region, in which multiple reflections accompanying resonance increase effective interactions between particle and wave. Moreover, in slot antenna

array, horizontal- and vertical-interactions between two adjacent slot antennas will be experimentally and theoretically explored.

Keywords : terahertz spectroscopy, terahertz nano-slot antenna, nano-particle detection, terahertz modulation, light-matter interaction, sub-skin depth barrier

Student Number : 2006-22905

Table of contents

List of figures

Chapter 1 Introduction

Optical properties of metallic subwavelength apertures have strongly been focused in near infrared and visible frequency regimes after the report by Ebbesen and his coworkers on extraordinary transmission of light via surface plasmon polariton.[1-4] Even in lower frequencies where most metals are considered as perfect electric conductor (PEC), it has theoretically and experimentally been studied that the transmitted electric fields through half-wavelength slot antennas are substantially enhanced when the thickness and the width of slot antennas are both in extreme subwavelength region.[5-8] These phenomena are attributed to their shape resonance with a large aspect ratio contributing the strong field enhancement inside the slot.[9-12] Recent researches on terahertz (THz) metamaterials in the sub-skin depth limit ($<\delta$) showed two complementary features: a giant electric field enhancement inside a gap with sub-skin depth spacing and the diminishing electric field enhancement with the thickness below $\delta/5$.[13-17] Based on these complementary properties in the sub-skin depth region, hereby one significant question is whether electromagnetic waves through resonant structures can be more sensitively controlled by *sub-skin-depth wide* metallic nano-objects to achieve new functionalities in tuning and detection applications.

Specifically, we have demonstrated control of the THz electromagnetic wave transmission by the metallic nano-scale objects, such as nano-barriers, nano-rods, and nano-particles, using THz nano-slot antenna with a hundreds micron length and a nano-sized width. The THz nano-slot antenna enhances electric field over the whole aperture, so that the *positions* as well as the *dimensions* of the nano-objects become important controlling parameters.[18] Interestingly,

when we put the single nano-objects inside or on top of the THz slot antennas, there are three different characteristics for each type of the nano-objects. Using a quantitative theoretical modeling based on a modal expansion, we provide a simple and intuitive picture that reveals the physical origin of these observations. Furthermore, we also show experimental evidence on how the same concept can be applied to detect a single gold nanoparticle embedded in a slot antenna in the millimeter wavelength region.

Chapter 2 Sample fabrications

2.1 Fabrication of nano-slit and –slot using Focused Ion Beam (FIB)

Focused Ion Beam (FIB) system use a focused beam of gallium (Ga^+) primary ions that can be operated for milling and imaging with a 5 nm resolution at low beam current.[19] Recently, FIB machine is widely used for fabrication of nano-sized patterns into a metallic film. Fig. 2.1(a) shows the images of our FIB machine, Quanta 3D (FEI), with a Scanning Electron Microscopy (SEM) and a FIB. A gold film is deposited onto a silicon or quartz substrate by thermal or electron-beam evaporation with a 5 nm-thick titanium or chromium adhesion layer. In order to fabricate an infinitely long nano-slit (Fig. 2.1(b)), 5 μm-long rectangular holes with a width of 70 nm are vertically stitched to produce a 3 mm long nano-slit, having the same width. This method helps us to overcome the limitation of the field of view in our FIB machine.

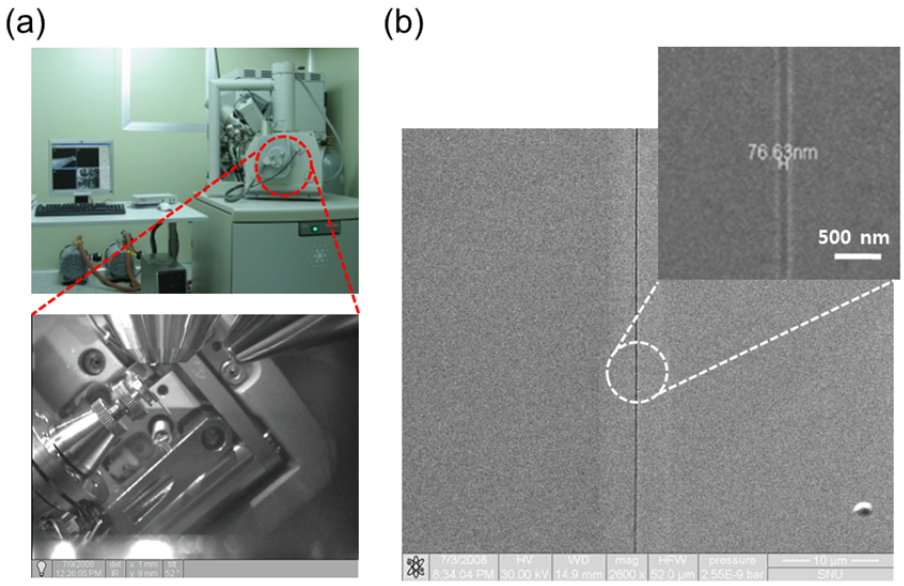

Figure 2.1 (a) The actual images of our FIB machine, Quanta 3D (FEI), with a Scanning Electron Microscopy (SEM) and a Focused Ion Beam (FIB). (b) The SEM pictures of an infinitely long nano-slit with the length of 3 mm and the width of 70 nm into a 60 nm-thick gold film, fabricated by the FIB.

2.2 Measurement of the cross-section of THz nano–slot antennas using FIB

Using the FIB machine, it is available to check the cross-section of the THz nano-slot antennas fabricated by FIB. The detailed processes by FIB are the following. First of all, we perform an electron-beam platinum (Pt) deposition with the beam current of 50~1500 pA, voltage of 5 kV, X=12 μm, Y=1 μm, Z=20 nm, the duration time of 3-5 minutes and the tilting angle of 0° onto the surface of the sample due to the protection of the sample surface. After that, ion Pt deposition with ion beam voltage of 30 kV, current of 0.1-0.5 nA, X=12

μm, Y= 1 μm, Z=2.5 μm, and the duration time of 1-2 minutes is performed at the 52° tilting angle of the sample stage. Using Regular Cross Section Milling option in FIB (Quanta 3D FEG, FEI) with the ion beam current of 3-20 nA, voltage of 30 kV, X=13 μm, Y=7 μm and duration time of 3-4 minutes, the bottom region (13 μm by 7 μm) of the Pt protection can be drilled. Finally, using Tilting Milling option in FIB with the ion beam current of 1-5 nA, voltage of 30 kV, X=13 μm, Y=2 μm, and the tilting angle of 53.5°, the intermediate region between the Pt protection region and the drilled hole region is also drilled due to the cleanness of the cross-section of the sample. Figure 2.2 shows the SEM image of a THz nano-slot with the length of 100 μm, the nominal width of 600 nm, and the metal thickness of 300 nm on the Si substrate, fabricated by FIB. Interestingly, there exist some damages caused by FIB milling at the substrate side below the slot area. Due to the substrate damages, FIB milling would be not suitable for making nano-slot antennas on a thin film with hundreds of nanometers thickness, such as a 100 nm-thick VO_2 film.[20-23] When we make THz slot antennas on the 100 nm-thick VO2 thin films, lift-off process using electron beam lithography would be one of the best solutions until now.

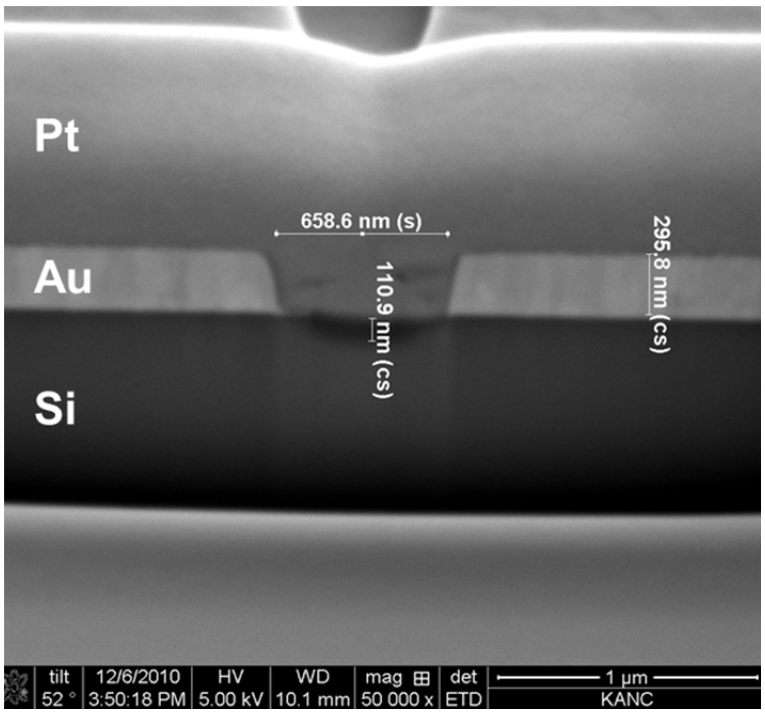

Figure 2.2 The SEM picture of a cross-section of a terahertz nano-slot with the length of 100 μm and the nominal width of 600 nm into a 300 nm-thick gold film, fabricated by the FIB.

2.3 Fabrication of nano-slot antenna array using electron-beam lithography

Fig. 2.3(a) depicts a schematic diagram of nano-slot antenna array into a thin gold film on silicon (Si) or silicon oxide (SiO) substrate. The nano-slot antenna array has the dimensions with hundreds micron length (*l*) and hundreds nanometer width (*w*). In order to fabricate a number of nano-slot antennas with the extreme aspect ratio of about 1000, we introduce a severe technique with higher resolution requirements, such as electron-beam lithography with field electron emission sources. Electron-beam lithography is

recently used as a powerful tool for nanotechnology architecture and integrated circuits. Fig. 2.3(b) depicts schematics of the fabrication process using negative photoresist (MA-N 2405). MA-N 2405 resist is spin coated with a 500 nm thickness (The resist thickness is determined to about 5~7 times thicker than the metal film thickness) on SiO substrate with the following conditions: 5000 rpm, 35 seconds, and 2.5 Acc. Then, the spin coated resist is baked by hot plate at 90 ℃ for 2 minutes 30 seconds. The baked photoresist is subsequently exposed by the scanning electron beam (with Acc. voltage of 25 kV and current of 30 pA) with the lithography program, NPGS. For development of the MA-N 2405 resist, the sample is dipped into the developer solution of MA-D 525 for about 1 minute 30 seconds. After that, the sample is cleaned by DI water and dried by nitrogen gas. Next, gold films with the 5 nm-thick chromium adhesion layers are deposited onto the photoresist pattern. Finally, gold nano-slot antennas are generated by a lift-off method with N-methyl-2-pyttolidone (NMP) solution at 70~80 ℃ for below 3 minutes (especially, below 2 minutes for Si substrate).

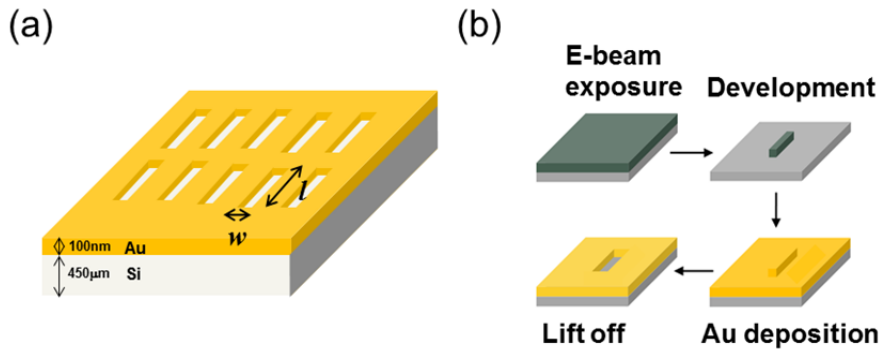

Figure 2.3 (a) Schematic of nano-slot antenna array in a gold thin film onto a Si substrate. (b) Schematic diagram of the electron-beam lithography process: electron-beam exposure, development, gold deposition, and lift off.[13]

2.4 Fabrication of platinum nano-rods using FIB

FIB machine has an additional tool, a deposition system, allowing the addition of material instead of removing material. This technique is realized by a gas delivery needle, supplying a chemical compound close to the interest point on the surface, as shown in Fig. 2.4(a). The chemical gas compounds consist of metallic-organic molecules, such as $(CH_3C_5H_4)(CH_3)_3Pt$ (for Pt), and $W(CO)_6$ (for W). These compounds will decompose locally and deposit Pt (or W) onto the surface when the compounds are exposed to the ion beam. Using this technique, the metallic nano-structures with the minimum size of around 50 nm can be realized without complex mask structures, even though the purity and conductivity of the material are usually lower than the pure metal.

We have applied this technique of FIB to the fabrication of Pt nano-rods onto the THz nano-slot antenna. For example, Fig. 2.4(b) shows a Pt nano-rod with the length of 1.5 μm, the width of 250 nm, and the thickness of 250 nm at the mid-point over the THz nano-slot antenna with the length of 150 μm and the width of 500 nm in a 100 nm-thick gold film. The Pt deposition method in FIB has the advantage of putting nano-rods at the desired locations over the nano-slot. Using this method, we studied on tuning of the resonance of THz nano-slot antenna depending on the locations of the Pt nano-rods, which will appear in the “chapter 6 terahertz pinch harmonics”.

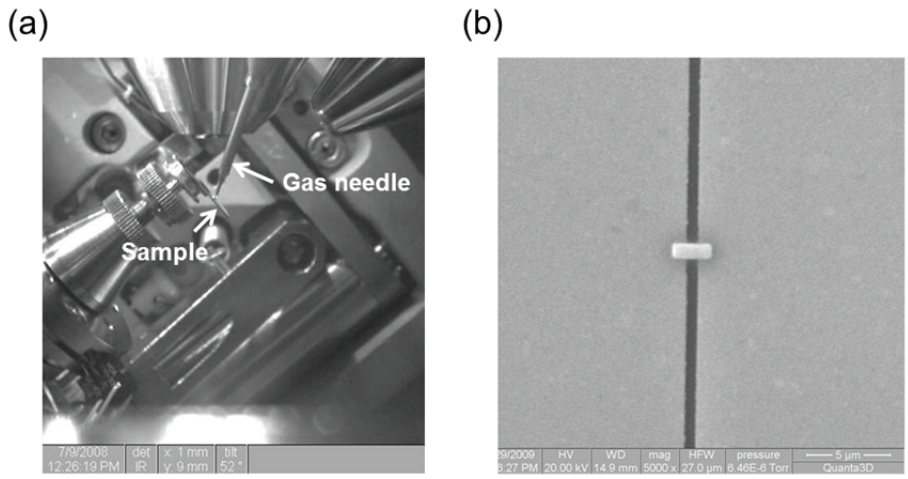

Figure 2.4 (a) Optical microscope image with the gas delivery needle and sample stage in FIB is shown when we deposit material on the sample. (b) The SEM picture of a platinum nano-rod with 1.5 μm length, 250 nm width, and 250 nm thickness onto a THz nano-slot antenna with the length of 150 μm and the nominal width of 500 nm into a 100 nm-thick gold film.

Chapter 3 Terahertz time-domain spectroscopy

3.1 Transmission-type THz time-domain spectroscopy

We perform transmission-type terahertz time domain spectroscopy in a frequency range from 0.05 THz to 2.0 THz with a single-cycle terahertz source generated from a 2 kV/cm biased semi-insulating GaAs emitter illuminated by a femtosecond Ti:sapphire laser (MIRA, Coherent) pulse train of a center-wavelength 780 nm, a 76 MHz repetition rate and a 130-fs pulse width (Fig. 3.1).[13,24,25] The spot size of terahertz wave at the focus point is about 3 mm, obtained by knife-edge experiment. By Fourier-transforming the time domain data, transmitted amplitude spectra for our sample, $E_{sample}(\omega)$, are obtained with phase information intact. For normalization of the measured spectrum, we use a reference signal, $E_{ref}(\omega)$, for the bare substrate after passing through 2 mm by 2 mm or 1 mm by 1 mm metal apertures.[26] We define the normalized (transmitted) amplitude ($T(\omega)$) against the aperture field as the ratio between two measured amplitudes:

$$T(\omega) = \left| E_{sample}(\omega) / E_{ref}(\omega) \right|.$$

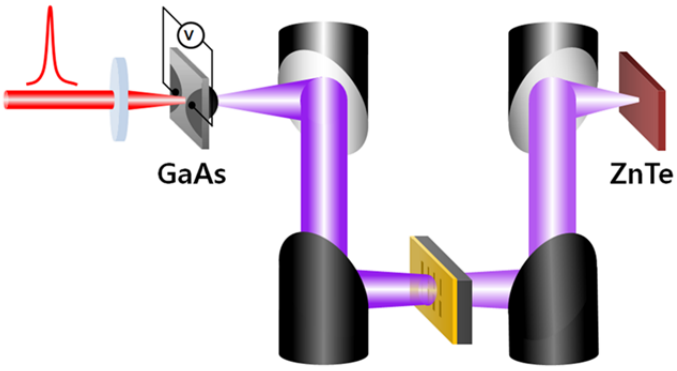

Figure 3.1 The schematic of our transmission-type terahertz time-domain spectroscopy with the GaAs emitter and ZnTe detector.[13]

3.2 Tight-focusing THz time-domain spectroscopy

For detecting a tiny signal of transmission through a single THz nano-slot antenna with the coverage ratio of about 0.001 %, we add Tsurupica lens (invented by RIKEN) to our THz setup for tightly focusing terahertz wave, as shown in Fig. 3.2. These THz lens help us to decrease the spot size at the focal point to below 1 mm, enhancing the THz electric field amplitudes by one order of magnitude compared with that of our old THz setup using the parabolic mirror. Using this new THz setup, we can obtain the transmission spectra of a single nano-slot antenna and look forward to observing an interaction between a single nano-particle and a single nano-slot antenna.

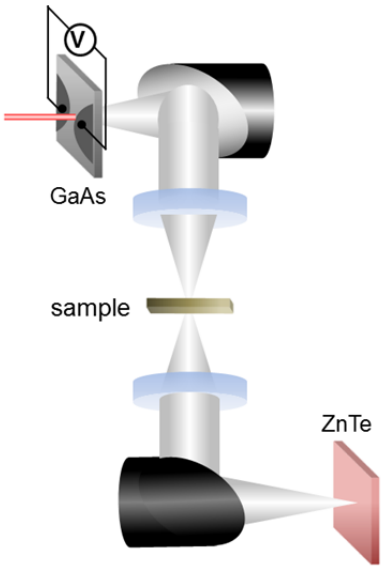

Figure 3.2 The schematic of the tight-focusing terahertz time-domain spectroscopy setup with the spot size of below 1 mm.

3.3 Broadband THz time-domain spectroscopy

For impulsive generation of broadband THz radiation, we used a commercial GaAs-based photoconductive THz emitter, Tera-SED (Gigaoptics, GmbH), instead of the hand-made photoconductive emitter in the tight-focusing THz time-domain spectroscopy setup.[27] For comparing the two emitters, their biased voltages are 125 V (Home-made emitter) and 50 V (Tera-SED3), respectively. Figure 3.3 shows that the new Tera-SED3 emitter generates a THz signal with a relatively shorter pulse width in the time domain and larger bandwidth in the frequency domain, compared to the hand-made emitter. We also find that the Tera-SED3 emitter has a greater advantage with higher electric field amplitudes in the frequencies of over 1 THz.

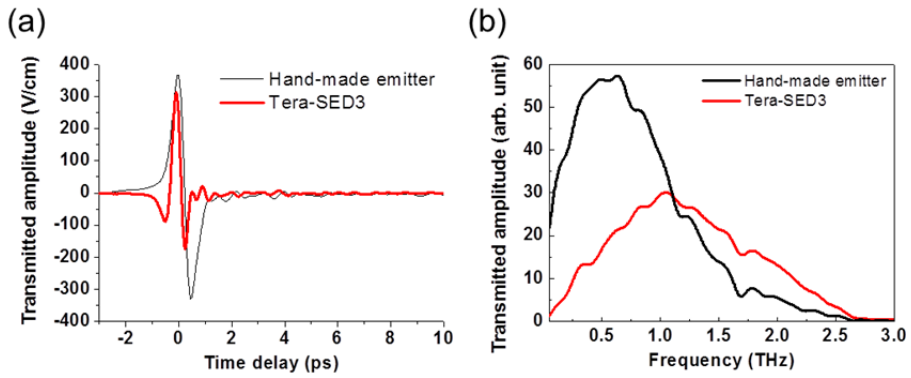

Figure 3.3 (a) Transmitted electric field amplitudes for the Hand-made emitter and Tera-SED3 in the time domain are shown as black and red curves, respectively. (b) Transmitted electric field amplitude spectra for both of emitters are shown in the frequency domain, respectively.

3.4 Dual-type THz time-domain spectroscopy

When we perform a quantitative absorption measurement, it is required to measure both of reflection and transmission through samples. What to use for this requirement is a Dual-type THz time-domain spectroscopy, being available to measure both of reflection and transmission through samples on a fixed sample loader. Figure 3.4 shows the layout of our Dual-type THz time-domain spectroscopy setup using a multi-pass THz beam splitter. The material of the THz beam splitter is HRFZ-Si. This beam splitter provides transmission/reflection ratio, 54/46 (%), in the wide wavelength ranging from 100 to 1100 μm. For avoiding a multiple reflection effect inside the beam splitter, we used the 3.5 mm-thick THz beam splitter, being relatively thick in the THz region.

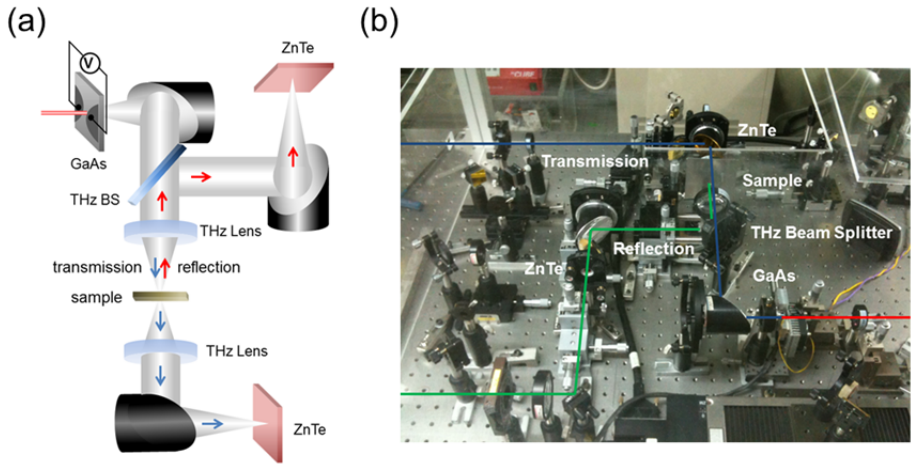

Figure 3.4 The experimental layout of the setup (a) The schematic presentation of our dual-type THz time-domain spectroscopy (b) The working setup in our laboratory.

For example, using this dual-type THz setup, we measured the reflection and transmission amplitude spectra of THz nano-slot antenna array with the length of 90 μm, the width of 50 nm, the horizontal period of 90 μm, and vertical period of 100 μm in a 50 nm-thick gold film on quartz substrate, as shown in Fig. 3.5. This dual-type THz setup would be applied to measure the absorption of chemical or biological molecules inside the nano-slot in the terahertz frequencies.

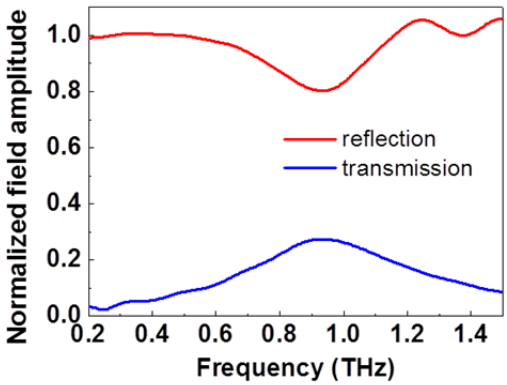

Figure 3.5 Reflection and transmission amplitude spectra of THz nano-slot antenna array with 90 μm length, 50 nm width, 90 μm horizontal period, and 100 μm vertical period in a 50 nm-thick gold film on quartz substrate are obtained by the dual-type THz time-domain spectroscopy setup.

Chapter 4 Terahertz nano-slot antenna

4.1 Introduction

THz nano-slot antenna means a rectangular hole with hundreds micron length and a nano-sized width in a thin metallic film, acting as a slot antenna with the resonance in a terahertz frequency region. At its resonance, the electric field enhancement inside the slot antenna increases as the slot width decreases due to shape resonance phenomena in metallic rectangular hole structures.[5,7,13,28] Recently, it was reported that one-dimensional nano slits with the width much smaller than their skin depth enhances electric field by orders of magnitudes with resonance-less 1/f frequency dependence.[26] So we investigate whether the THz nano-slot antennas with sub-skin depth wide widths also allow a huge enhancement of the electric field particularly at resonance. Moreover, horizontal coupling between two adjacent slot antennas as well as substrate effect on the resonance of the slot antennas, caused by strong local field around each slot, will be also explained in this chapter.

4.2 Single THz nano-slot antenna

In this section, we show that a single THz nano-slot antennas with hundreds micron length (l) and nano-meter sized width (w) funnels terahertz electromagnetic waves through, accompanied by a large field enhancement unavailable for micron-scale aperture widths (Fig. 4.1(a)).[29] With the slot width and film thickness close to the skin-depth, theory based on the perfect conductor approximation still gives good agreement.[30] With the ultrathin metal film much smaller than the skin depth, we achieve essentially a giant

field enhancement of over 1000 inside the slot at the resonance.[30]

We first consider single nano-slot antennas in a gold film with 100 nm thickness (t) on a dielectric substrate of 0.5 mm-thick quartz crystal. These terahertz nano-slot antennas, patterned by FIB, in dimensions of the length l=150 μm and the various widths of w=120, 240, 500, 1000, and 5000 nm enhance transmittance at the resonance frequency of 0.55 THz, which is $\sim c/(2n_{eff}l)$ where n_{eff} the effective refractive index of the substrate and c the velocity of light in vacuum.[31,32]

To obtain normalized transmitted amplitude through the THz nano-slot antennas, we perform terahertz time domain spectroscopy in a frequency range from 0.2 THz to 1.2 THz. By Fourier-transforming the time domain data, transmitted amplitude spectra for our sample, $E_{sample}(\omega)$, are obtained with phase information intact. For normalization of the measured spectrum, we use a reference signal, $E_{ref}(\omega)$, for the bare substrate after passing through a 1 mm by 1 mm aluminum aperture. We define the normalized-to-area amplitude against the aperture field as the ratio between two measured amplitudes, equal to the average enhancement of the electric field inside the slot, using a normalizing aperture of 1 mm by 1mm dimensions:

$$\text{Normalized}-\text{to}-\text{area amplitude} = \left|E_{sample}(\omega)/E_{ref}(\omega)\right| \times \frac{1}{\text{coverage ratio}} .$$

Figure 4.1(b) renders the normalized-to-area amplitude spectra as measured for five different slots, having the widths (w) ranging from w=120 to 5000 nm. Especially, we observe the strong field enhancement of over 1000 characterizing THz slot antennas with extremely large aspect ratio of 1250 for

the width of 120 nm. This giant field enhancement helps measuring the transmission through only a single nano-slot antenna using our far-field transmission setup with the signal-to-noise ratio of over 10000, even though the coverage ratio of the single slot is about 0.0018 %. Single THz nano-slot antenna with a giant field enhancement opens a strong possibility of potential applications, such as nanoparticle detection[33,34], nonlinear,[35-38] and active switching devices.[39,40]

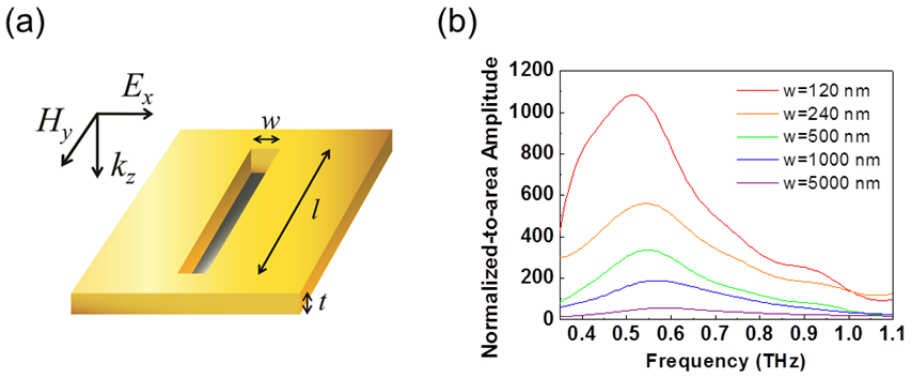

Figure 4.1 (a) Schematic of a single THz nano-slot antenna with a length of *l* and a width of *w*. (b) Experimental normalized-to-area amplitude spectra of single THz slot antennas with a length of *l*=150 μm and various widths of *s*=120, 240, 500, 1000, and 5000 nm.

4.3 Terahertz nano-slot antenna array: Ultra-broadband performance

In this section, we consider an array of THz nano-slot antennas, having dimensions with 100 μm*200 nm (*l***w*), in a metallic film with 100 nm thickness on a dielectric substrate of 450 μm-thick undoped silicon. These THz nano-slot antennas enhance transmittance at the resonance frequency of

0.6 THz. We pattern these nano-slots by electron beam lithography using a negative photo-resist and the single-layer lift-off process. This fabrication method allows access to an extreme ratio rectangular hole with a sub-micron sized width preserving a hundred micron-sized length.

THz nano-slot antennas with varying period d_x are investigated with polarization of the normally incident light perpendicular to the length direction. Scanning electron microscope (SEM) pictures with the top view of these samples are shown in the insets of Figs. 4.2(a)-4.2(b). In Fig. 4.2(a) and 4.2(b), experimental results are the normalized amplitude spectra for the period of 100 μm (coverage ratio of 0.18 %) and 30 μm (coverage ratio of 0.6 %), with the same length (l=100 μm) and width (w=200 nm). When the horizontal period decreases to 30 μm, the normalized transmitted amplitude increases to over 90 % at the resonance despite the still small coverage of only 0.6 %. However, with micro-patterned samples, where it was reported that to preserve normalized transmitted amplitude of over 90 %, slot coverage of over 12% was needed.[41,42] While the field enhancement for the micro-gap rectangular hole array was only 8,[7,41] that for the nano-slot array with the areal coverage of 0.6 % is over 150. This nano-sized gap slot samples have a good advantage of retaining the antenna cross section, being relatively insensitive to the decreasing the width compared with the micron-sized gap samples. Furthermore, decreasing horizontal period also induces to push the Rayleigh minima out of the measurement range, again contributing to the enhanced transmission.[43] In Fig. 4.2, it should be also noted that the line width of the transmitted curve with higher coverage sample (Fig. (4.2(b)) is noticeably larger than that for the low coverage sample (Fig. 4.2(a)).

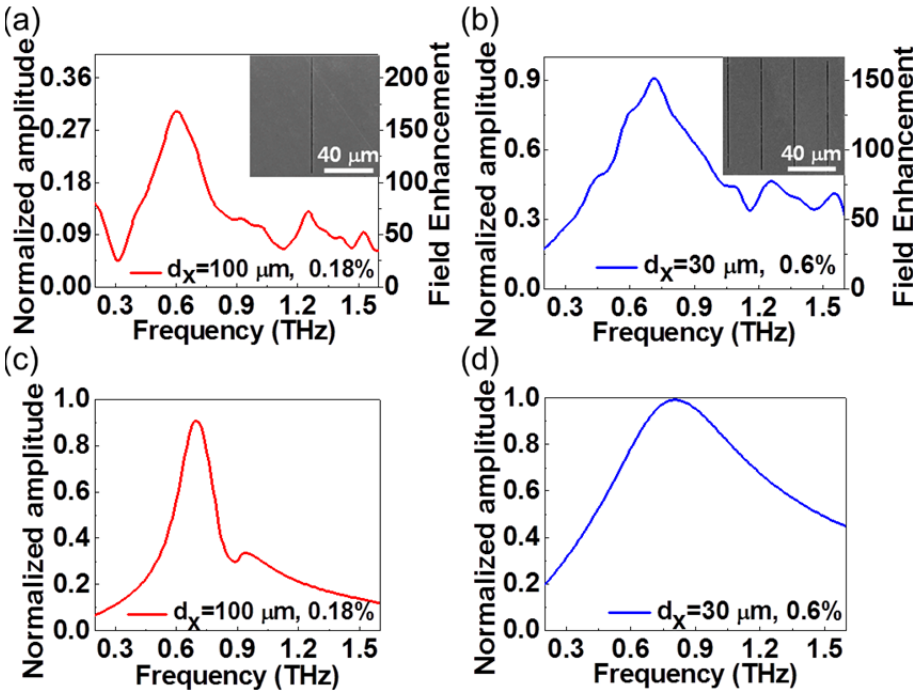

Figure 4.2 (a) Normalized transmitted amplitude spectra measured through an array of nano-slot antennas with a length l=100 μm, a width w=200 nm, and horizontal period d_x=100 μm and vertical period d_y=110 μm. (b) The same as (a) except d_x=30 μm. SEM images of the samples are shown in the insets. (c) A modal expansion based theoretical calculations with the period d_x=100 μm, and (d) d_x=30 μm.[13]

For better understanding the horizontal coupling between two adjacent slots, we introduce an analytical calculation based on modal expansion assuming perfect conductor and infinite array.[44] One more assumption is that we use the single mode approximation considering only the half-wavelength mode for each slot. Based on these assumptions, we obtain the zeroth order normalized transmitted amplitude (T_0) at normal incidence as the following:

$$T_0 = \left(\frac{n+1}{2n}\right)\frac{2wl}{\pi d_x d_y}\frac{\dfrac{4i\mu}{k\pi}}{\left(W^2+\left(\dfrac{2\mu}{k\pi}\right)^2\right)\sin\mu h + 4\dfrac{i\mu}{k\pi}W\cos\mu h},$$

where d_x, d_y are periods along the x and y directions respectively, n the refractive index of substrate, k the wave vector of the incident light, h the thickness of metal, μ the waveguide vector, $\mu^2 = k^2 - (\pi/l)^2$, and finally W the self-illumination term describing coupling of the hole-eigenmodes with the incident wave.[28,31,42,45]

In Fig. 4.2(c) and 4.2(d), the transmission curves obtained by our analytical solutions are in good qualitative agreement with our experimental results. Especially, even though the used metals in experiments are considered as perfect electric conductor, our theoretical approaches still capture the essential physics, including the increasing line width and blue-shift of the peak position with decreasing period. However, for the 100 μm period case, the normalized amplitude value shows noticeable disagreement between the experimental and theoretical results, most likely due to the small number of nano-slot antennas in each direction: only nine.[46,47] Despite this disagreement, we emphasize that the broadband performance enabled by decreasing the period is well explained in both of the experiment and theoretical model and the slot array with single resonance may not give enough bandwidth.[42,48] So we can guess that the new slot array with multiple resonances, including different length slot antennas, would provide the bandwidth encompassing all fundamental resonances corresponding to each length.

Here, we show an elegant way to achieve the ultra-broadband performance

using a multi-antennas-per-unit cell idea, in the broad range from 0.2 to 2.0 THz. The unit cell structure borrows the concept of log-periodic antennas introduced by DuHamel and Isbell.[49,50] In our unit cell, ten THz nano-slot antennas with four different lengths are contained, as shown in Fig. 4.3(a). The design rule is that: l_1=200 μm, l_2= l_1/2=100 μm, l_3= l_1/3=67 μm, l_4= l_1/4=50 μm, with all antennas having the same width of 250 *nm*. To maintain the same coverage for each antenna length, we have four antennas in column with l_4= 50 μm, three antennas with l_3=67 μm, and two antennas with l_2=100 μm. The spacing between the adjacent two antennas is arranged such that s_1=2s_2=4s_3. We consider two structures with different periods: d_x=110 μm; s_1=40 μm and d_x=40 μm; s_1=15 μm, with the unit cells denoted by solid lines in Fig. 4.3(b). In Fig. 4.3(c), the normalized amplitudes for the samples show ultra-broadband spectra of over 3 octaves spanning from 0.2 to 2.0 THz. In the case of the period d_x=40 μm, the period pushes the Rayleigh minima out of our spectral range of the four fundamental resonances (0.35 THz, 0.7 THz, 1.1 THz and 1.5 THz) for each length of nano-resonator, resulting in about 70% of normalized amplitude over the whole spectral range. With the recent introduction of active terahertz metamaterials controlled by an external stimulus,[39,40,51,52] log-periodic THz nano-slot antennas can provide further progress towards ultra-broadband active metamaterials.

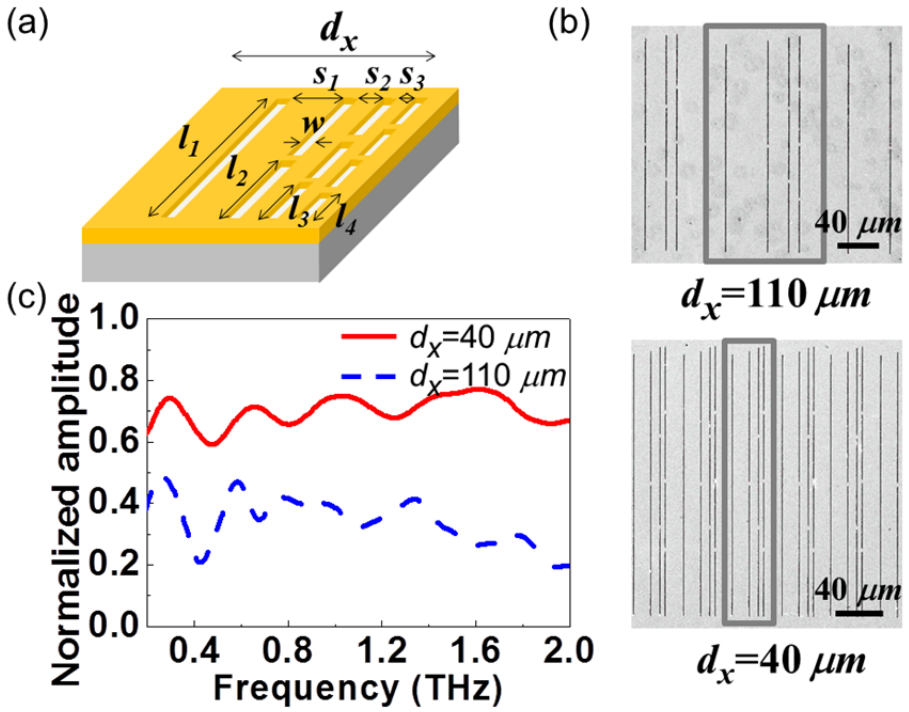

Figure 4.3 (a) Schematic of log-periodic terahertz nano-slot antennas with four different lengths (l_1=200 μm, l_2=100 μm, l_3=67 μm, l_4=50 μm), three different spacings (s_1, s_2, s_3), and the same width (w=250 *nm*). (b) SEM images of the two samples with different periods: d_x=110 μm (s_1=40 μm, s_2=20 μm, s_3=10 μm) (top) and d_x=40 μm (s_1=15 μm, s_2=7 μm, s_3=4 μm) (bottom). Solid line boxes denote a unit cell in each structure. (c) Normalized amplitude spectra measured through the two samples with different periods of 110 μm (dashed line) and 40 μm (solid line) in the range between 0.2 and 2.0 THz.[13]

4.4 Substrate effect on the resonance of THz nano-slot antenna array

In this work, we show that resonance behaviors of a single THz nano-slot

antenna perforated in a thin metallic film on a finite dielectric substrate depend on the substrate thickness as well. The earlier works of freestanding single slot antennas in PEC showed that the resonance peak position slightly shifts to lower frequencies (red-shift) as increasing the width.[53,54] On the other hand, as the substrate thickness is reduced to several microns, the resonance frequency is clearly blue-shifted for the increasing the slot width where Ohmic loss in metal plays an important role.[55,56] We also demonstrate these resonance shifts can be seen not only in real metal but in perfect electric conductor (PEC) cases.[32] All in all, the substrate thickness and the slot width in the extreme subwavelength limit are additional crucial factors determining the resonance frequency of THz slot antennas on a finite substrate.

We experimentally study resonance behaviors of slot antennas in two different cases. Slot antennas with a fixed length (l=150 μm) but different widths are perforated in a 60 nm-thick gold film deposited on a combined 2 μm -thick SiN/SiO2 substrate (Fig. 4.4(a)) and on a Si substrate with 500 μm thickness (Fig. 4.4(b)), respectively. Our slot antennas with various widths (150 nm, 500 nm, 1 μm, 2 μm, and 5 μm) are investigated with the normally incident light with polarization parallel to the width direction. Scanning electron microscope (SEM) images of these samples are shown in Fig. 4.4(c).

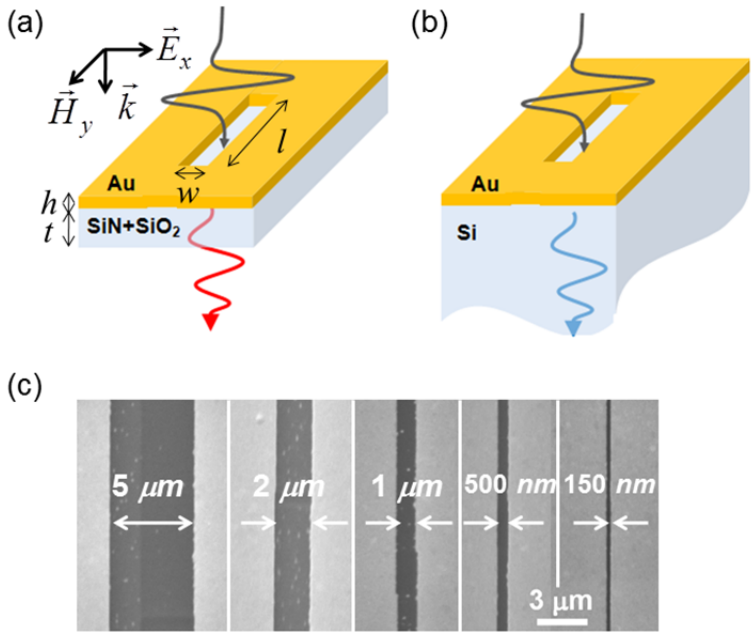

Figure 4.4 (a) Schematic diagram of a single slot antenna in a gold film on a finite substrate (SiN+SiO_2), including the spatial dimensions. (b) A slot antenna with a 500 μm thick Si substrate. (c) SEM images of slot antennas with diverse widths (w = 5 μm, 2 μm, 1 μm, 500 nm, and 150 nm).

In Fig. 4.5(a) and 4.5(b), we presented transmittances of slot antennas on the 2 μm thick SiN substrate and on the 500 μm thick Si substrate, normalized by transmittances through each bare substrate. The resonance peak positions on two substrates commonly shift to higher frequencies (blue shift) for increasing width, as a real metallic feature of the thin gold film in THz frequencies. Especially, the resonance frequency difference between the narrowest and the widest slot on the 2 μm thick SiN substrate is larger than that on the 500 μm thick Si substrate.

We also perform three-dimensional finite difference time domain (FDTD) simulations[57-59] and obtain the enhancement of transmitted electric fields

through different widths of rectangular holes (w = 150 nm, 500 nm, 1 μm, 2 μm, and 5 μm) on two substrates, 2 μm thick SiN and 500 μm thick Si substrates. For Fig. 4.5(c) and 4.5(d), the metal film is considered as real metal (gold) with thickness h = 60 nm. The FDTD simulations show good agreements with corresponding experimental results in Fig. 4.5(a) and 4.5(b).

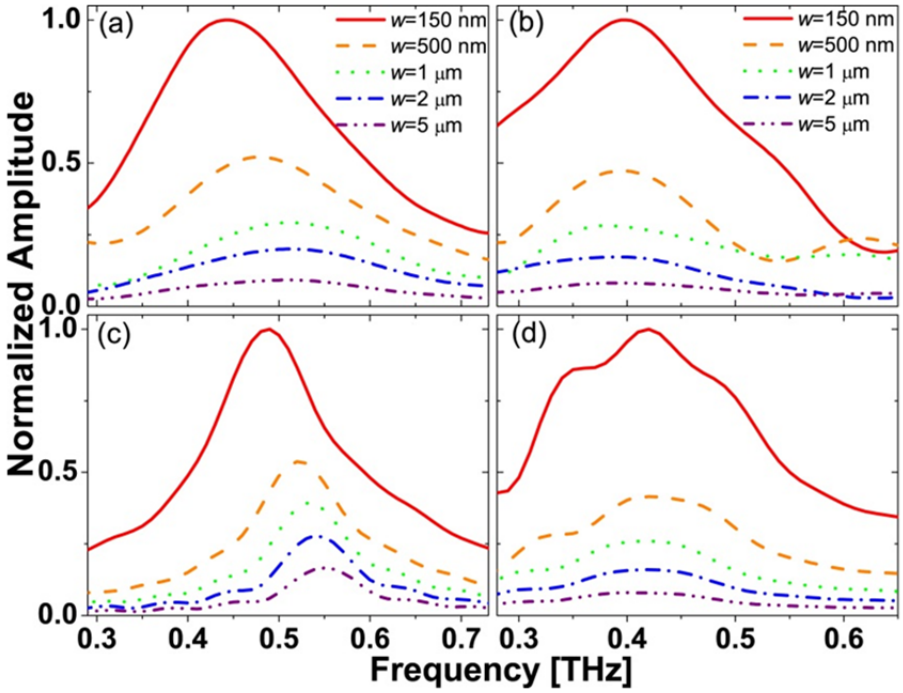

Figure 4.5 (a) Normalized transmitted amplitude spectra measured through slot antennas with length l=150 μm, and different widths w=150 nm, 500 nm, 1 μm, 2 μm, and 5 μm on the 2 μm thick SiN substrate. (b) The same as (a) but with a 500 μm thick Si substrate. (c) The FDTD simulations for SiN, and (d) for Si substrate.[32]

For better understanding fundamental physics of such resonance behaviors on dielectric substrates with different thickness, we perform the modal expansion model although the finite substrate effect is missing.[5,55] For a slot antenna

perforated in an extremely thin metal film, the resonance frequency and the spectral broadness of the transmitted field are determined by the real and the imaginary value of the self-radiation, respectively, and the self-radiation is given by the in-plane modal integration of the Green function multiplied by the form factor of the slot antenna. The Green function is functionalized to multiple reflections of electromagnetic waves in the substrate, thereby independent from the slot antenna dimensions. The form factor means the Fourier-transformed expression of the slot antenna in mode space. For the narrow slot antennas, the form factors are constantly distributed over entire mode space, and the real value of the self-radiation has most contribution in evanescent modes,[31] thereby resonance frequencies of the narrow slot antennas are relatively insensitive to multiple reflections of the transmitted wave in a finite substrate, compared to those of the wider slot antennas.

Conclusively, we present the resonance behaviors of a single slot antenna perforated in a gold film on finite substrates. We find that the slot width and the substrate thickness are other crucial parameters for determining resonance behaviors of THz slot antennas on finite substrates, while the slot width has almost no influence on the resonance of freestanding metallic apertures. Moreover, when the substrate thickness decreases below 2 μm, the blue shift of resonance peak can be found in real metal film. We can apply our results to research area where sophisticated resonance frequency control is requested, such as active THz devices, filters, and bio-, chemical-, molecule analysis and detection.

Chapter 5 Strong coupling between slot antennas separated by sub-skin depth barriers

5.1 Introduction

The transmission properties of periodic arrays of slot antennas have been investigated where almost perfect transmission was explained by strong field enhancement inside the holes.[13,41,42] Furthermore, ultra-broadband THz transmission through periodic slot antenna arrays has been achieved with a deep subwavelength period of 2 μm, due to the strong coupling among horizontally aligned slots.[60] However, the coupling between vertically aligned slot antennas has generally been ignored, because the coupling between parallelized dipoles is relatively weak compared to that between serialized dipoles. Hereby one fundamental inquiry would be the threshold spacing between two vertically aligned slots, recognized as one single or two individual slots by an incident electromagnetic wave.

In this chapter, we experimentally demonstrate a nano-scale control of the coupling between two vertically aligned slot antennas with an extremely small separation between them, down to 5 nm. At large separations, constituting a hard boundary for the slots, a resonance f corresponding to the half-wavelength resonance of the two identical slots is found. As the separation decreases to the below skin depth level, the resonance is ultimately shifted to $f/2$: there exists a strong coupling between the slot antennas, so that they

essentially merge together to form a new fundamental mode.

5.2 Paired *positive* rod antennas vs. paired *negative* slot antennas

Recently, paired positive metallic nanostructures, such as, nanoshell,[61-63] nanorod,[64-66] and nanoparticles,[67-69] with air or dielectric nano gaps have received much attention regarding the field enhancement,[70] nanoparticle detection,[34,71,72] and pattern-tuning ability[73,74] in visible and infrared regimes (Fig. 5.1(a), left). At distances below 1 nm, a new resonance mode arising from electron tunneling through the air gap emerges[75,76] (Fig. 5.1(b), top). However, it is experimentally quite difficult to observe the *continuous* transition to the dipole resonance across the entire length of the nanostructure because of the problem on fabrication of sub-nanometer air gap with an accuracy of less than 0.1 nm.[75-77]

On the other hand, when we consider two vertically-aligned “negative” (slot) antennas (Fig 5.1(a), right) with a metallic nano-scale barrier, slots replacing metals and the metallic barrier replacing the air gap, another important length scale enters. The coupling between the paired slots changes drastically as the barrier width decreases from the skin depth (δ) to extreme sub-skin depth ($\delta/10$) (Fig. 5.1(b), bottom)- in this sense, the Babinet’s principle is not applicable when comparing antennas and slot antennas with sub-skin depth barriers. This is because the strongly enhanced resonant electric field inside each slot can penetrate through the sub-skin depth barrier, couple the adjacent resonant modes, and generate a new resonant mode. To use Maxwell’s correspondence, the sub-skin depth barrier cannot carry enough current to

completely separate the two slot antennas. The deep-sub skin depth regime, despite its vast potential for exploring fundamental physics and for unique device applications, has not been fully explored.

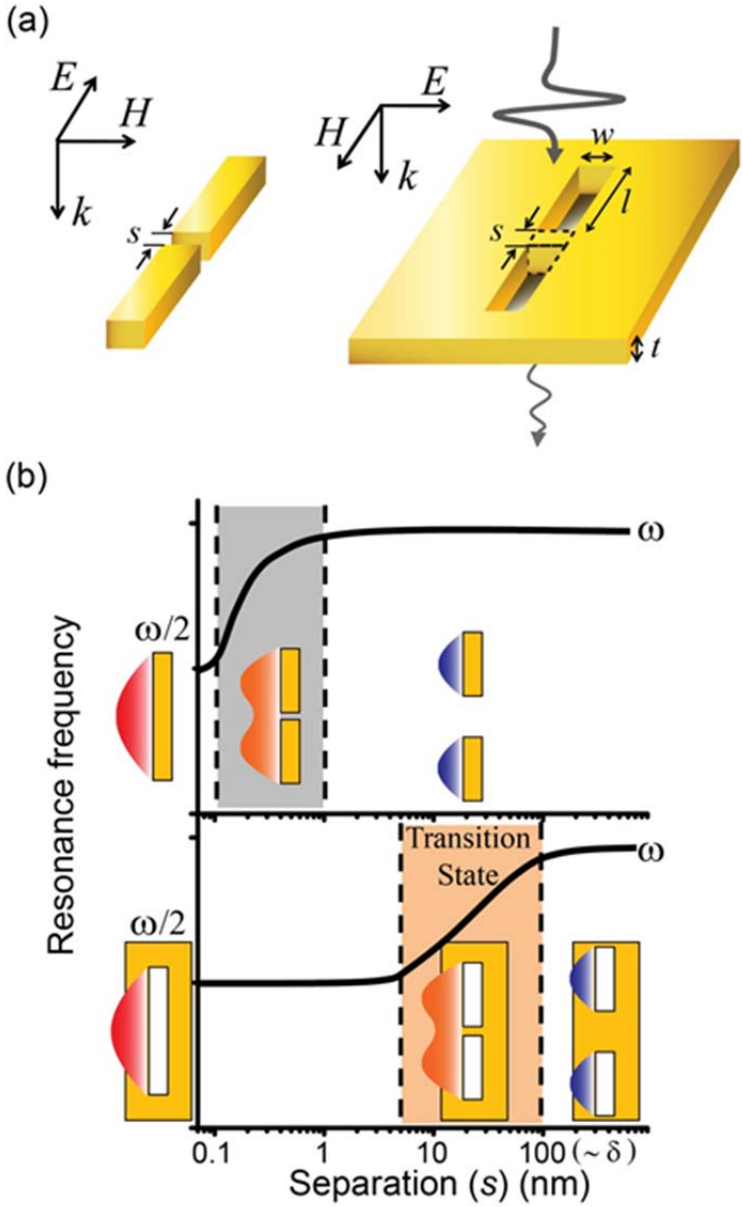

Figure 5.1 (a) Schematics of (left) an air nano gap width *s* between paired positive antennas and (right) a metallic nano barrier with width *s* between the paired THz slot antennas with a length *l* and a width *w* fabricated on a thin gold film with a thickness *t*. In the slot antennas, the p-polarized lights with polarization perpendicular to the long axis of the rectangle are normally incident on the sample. (b) The comparison between (top) positive antennas and (bottom) negative slot antennas making resonance transitions from the resonance at frequency ω of each individual antenna to the resonance at $\omega/2$ of the entire-length antenna, depending on the separation between the two antennas.[30]

5.3 Metallic nano barrier between the paired THz slot antennas

We measure transmission spectra of two vertically-aligned identical slot antennas in a frequency range from 0.1 THz to 1.0 THz using terahertz time domain spectroscopy. The slot antennas, patterned by focused ion beam, have dimensions of length *l*=150 μm and width *w*=120 nm in a gold film with thickness *t*=60 nm deposited onto a 2 μm-thick SiN/SiO_2 substrate (Fig. 5.2(a)). Nano barriers with mean widths of *s*=0, 5, 15, 50, 120, 220, and 410 nm separate the two equal-length slot antennas (Fig. 5.2(b)). Especially, the strong field enhancement of over 1,000 characterizing THz slot antennas with extremely large aspect ratio helps modulating the antenna resonance using the metallic nano barrier with nanoscale precision.

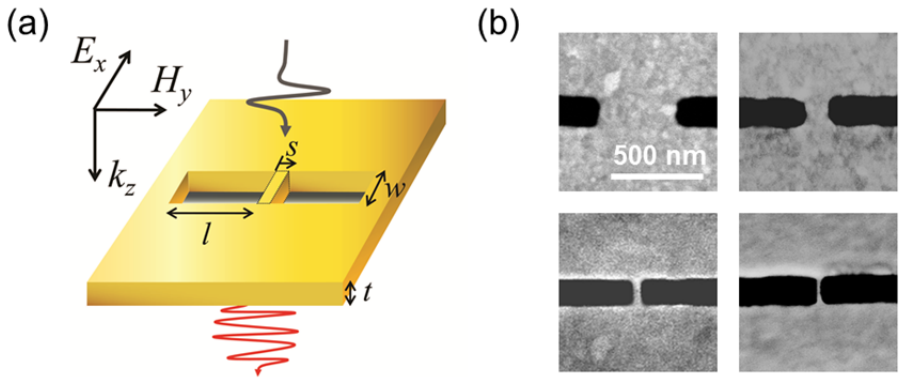

Figure 5.2 (a) A schematic of two slot antennas with a length *l* and a width *w* separated by *s*, fabricated on a thin gold film with a thickness *t*. (b) Enlarged scanning electron microscopy images of two slots with s=410 nm, 120 nm, 15 nm, and 5 nm.

In Fig. 5.3, we start to see significant red-shift in the resonant transmission peak already for *s*=120 nm close to the skin depth of gold (δ_{gold}=118 nm at 0.4 THz[14,78]). For the thinnest 5 nm-wide nano barrier we used, it is noted that the resonance frequency converges to that of a two-times-lengthened slot antenna. To our knowledge, this strong coupling result is the first observation of the continuous transition from the half- to the full-wavelength modes in a metallic nano-gap slot antenna.

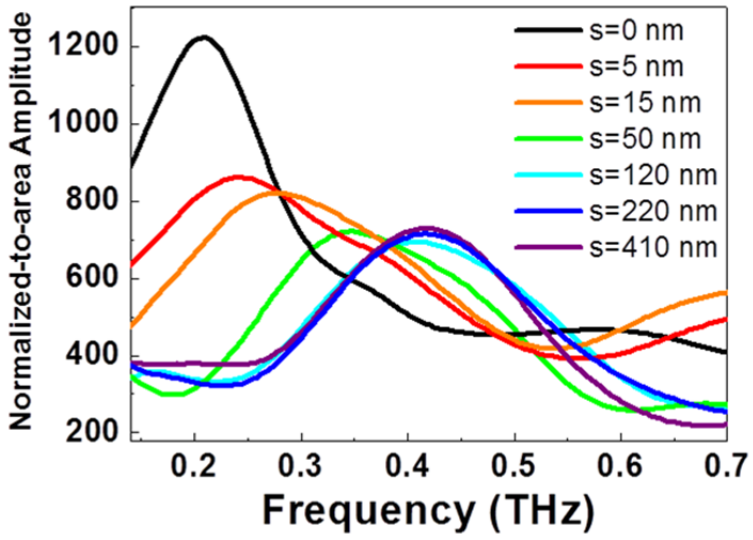

Figure 5.3 Experimental normalized-to-area amplitude spectra of two identical THz slot antennas (l=150 μm and w=120 nm) separated by various barriers of width s=0, 5, 15, 50, 120, 220, and 410 nm.[30]

For better understanding the physical origin of this evolution of the transmission spectra, we use a theoretical formalism based on a modal expansion of the electromagnetic fields in our structure.[5,6,44] It should be noted that our theoretical framework can accurately work with the extremely large aspect ratio of the slot antenna, about 2500, even though most of the standard tool used in nano-optics, such as the finite-difference time-domain (FDTD) method, has a limitation to solve this problem due to the combination of very different length scales. For applying our theoretical approach to the two paired slot antennas with the metallic barrier at the middle, we introduce the following two approximations: First, all external air-metal interfaces except the contact with the nano barrier are applied to perfect-metal boundary condition. We use a conventional Drude-like formula for the dielectric constant of the metallic nano barrier. Second, we only consider the

fundamental mode of the whole aperture.

Figure 5.4 shows the normalized-to-area transmitted amplitude as computed for the seven different samples considered in Fig. 5.3. As shown in this figure, there is a good agreement between the theoretical calculations and the corresponding experiments, both in the amplitude and the spectral position of the resonant transmission curve, in which no fitting parameters are used in our numerical calculations. There are slight discrepancies between theory and experiments, being attributed to the following facts. On the one hand, SEM images of several transversal cross sections of the nano barriers show that the actual shape of the nano barriers resemble a rectangular pyramid with rounded edges, not a perfectly rectangular block as considered in our theory. On the other hand, in our theory, we used conventional bulk parameters for gold at THz frequencies for simulating the electromagnetic response of the nano barrier by means of a Drude-like formula. However, several earlier works show that those parameters, such as the dielectric constants of the metal, can be changed in sub-skin depth metallic films.[57,58] We have also found that this effect is much larger for the thinner barriers considered in this work.

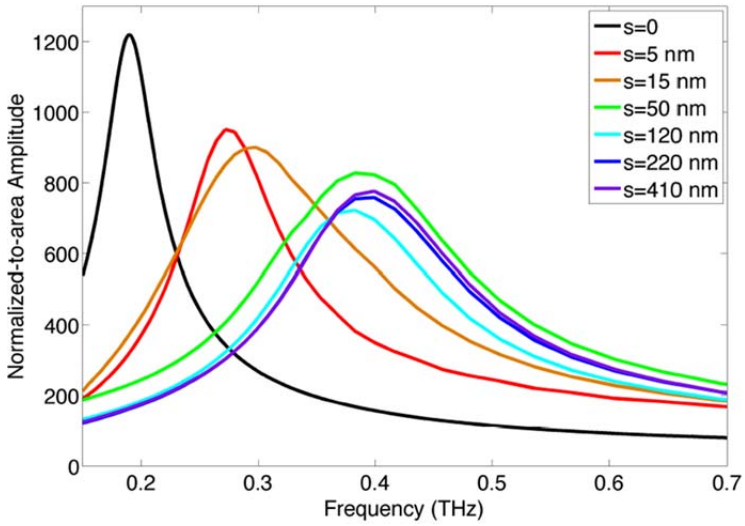

Figure 5.4 Normalized-to-area amplitude spectra numerically calculated for seven cases of the two identical THz slot antennas (l=150 μm and w=120 nm) considered in Fig. 5.3

5.4 Application

To apply our concept to the nanoparticle detection using terahertz waves, we investigate whether a metallic nanoparticle placed on top of a slot antenna can shift the resonance, all the way to separating the two cavities. We introduce platinum (Pt) nanoparticles placed on the top of the THz slot antenna with dimensions of a total length l=300 μm and a width w=120 nm (Fig. 5.4(a)). Pt nanoparticles are fabricated by Pt-deposition method using focused ion beam. Figure 5.4(b) shows normalized-to-area amplitude spectra, with the two nanoparticles at the center position, of the THz slot antenna with the fundamental resonance of 0.2 THz, as used in previous figures. A nanoparticle with 600 nm width at the mid-point turns off the fundamental, and generates a new resonance at twice the fundamental resonance frequency. A smaller

particle with 200 nm-width nanoparticle affects the resonance much less, although a sizable shift is noticeable. Comparison with nano barrier data indicate that the *effective* separation *s* introduced by a nanoparticle sitting on *top* of the aperture would be much smaller than its size, strongly suggesting that the resonance shift can be a very sensitive measure of the contact between the nanoparticle and the slot antenna.

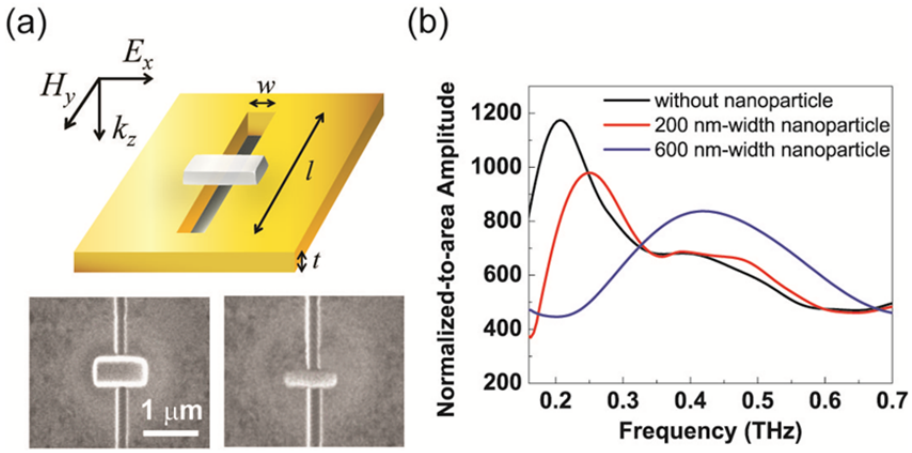

Figure 5.5 (a) A schematic of a platinum (Pt) nanoparticle *on* the THz slot antenna with dimensions of a total length *l*=300 μm and a width *w*=120 nm. An (top) SEM picture of a Pt nanoparticle with a length of 1 μm, a width of 600 nm, and a thickness of 400 nm, located at the center position on the THz slot antenna. At the bottom, an enlarged SEM image of a smaller nanoparticle with length of 1 μm, width of 200 nm, and thickness of 250 nm. (b) Normalized-to-area amplitude spectra of the THz slot antenna without nanoparticle, with the 600 nm-width, and 200 nm-width nanoparticles at the center position.[30]

5.5 Conclusions

We have presented that a sub-skin depth metallic barrier separating two vertically-aligned terahertz slot antennas allows strong coupling, forming a transition state between the full-wavelength and the half-wavelength states. Penetration of a diffracted light through the 5 nm wide nano barriers of the extreme sub-skin depth limit, ~δ/20, enables terahertz electromagnetic waves to be tailored by nano objects paving important paths towards ultra-sensitive tuning and detection using long-wavelength light

Chapter 6 Terahertz pinch harmonics

6.1 Introduction and Background

A pinch harmonic (or guitar harmonic) is a musical note produced by *lightly touching the thumb of the picking hand* upon the string immediately after it is picked.[79] This technique turns off the fundamental and all overtones except those with a node at that location. Here we present a terahertz (THz) analogue of pinch harmonics, whereby a metallic nanorod placed across a terahertz nano-slot antenna shifts or overdamps the resonance depending on the rod-size. Strikingly, smaller nanorods turn off transmission much more drastically than their larger counterparts. By modeling a nanorod inside a nano-slot, we show that THz pinch harmonics yielded by the nanorod with *sub-skin depth* dimensions can be qualitatively understood within a microscopic theory of the transmission through the hole.[80] Our work demonstrates that terahertz electromagnetic waves can be tailored by nano particles, paving important path towards THz switching and detection applications.

Hereby, we demonstrate a terahertz analogue of pinch harmonics (Fig. 6.1(a)) by placing a nano-sized obstacle in a THz nano-slot antenna.[18] We show that a single metallic nanorod (Fig. 6.1(b)) as an obstacle could select a specific higher mode or mute nearly all the resonance modes in the hundreds of micrometer length hole despite the rod's dimension being smaller than about $\frac{\lambda}{1{,}000}$, whereas a bigger metallic rod generate new fundamental modes.

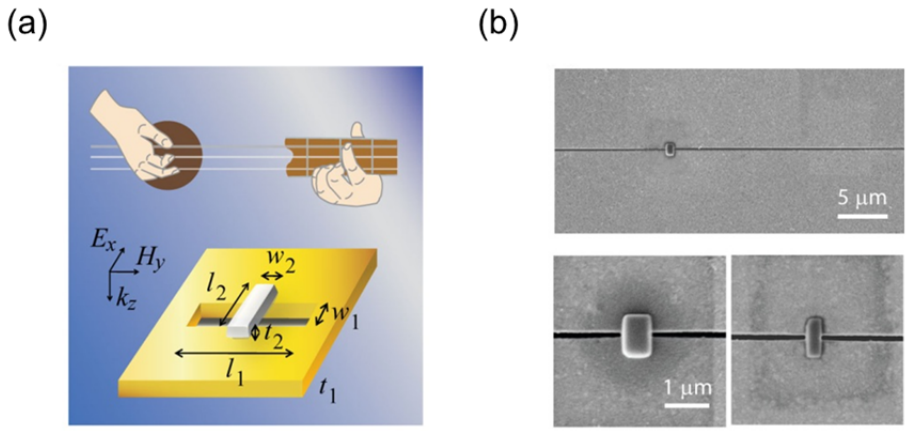

Figure 6.1 (a) Schematic diagram of a single nanorod on a THz nano-slot antenna. The p-polarized terahertz pulses with polarization perpendicular to the long axe of the rectangle are normally incident on the sample. (b) (top) An SEM picture of a larger nanorod with a length l_2=1 μm, a width w_2=600 nm, and a thickness t_2=400 nm at the 1:2 position on a THz nano-slot antenna (length l_1=300 μm and width w_1=120 nm). In the bottom, SEM images of an enlarged area around first larger nanorod (left), and second smaller nanorod (right) with l_2=1 μm, w_2=250 nm, and a thickness t_2=250 nm.[18]

For an ordinary pluck of a string, the resulting vibration is a superposition of standing waves: the first few modes (n=1, 2, and 3) are illustrated in Fig. 6.2(a). If we wish to have higher harmonic modes, we firmly place our finger at, say, the 1:2 position along the string, generating two different fundamental modes at each side, suppressing the original fundamental mode completely (Fig. 6.2 (b)). When the finger lightly touches the same position on the string, the third harmonic becomes the dominant mode, suppressing both the original fundamental mode and the new fundamental mode of the long side (Fig. 6.2 (c)). This technique is called ‘pinch harmonics’, being useful for fine-tuning a guitar. The concept of terahertz pinch harmonics is when the string is replaced

by the extreme-ratio nano rectangle and the finger by nanorods.

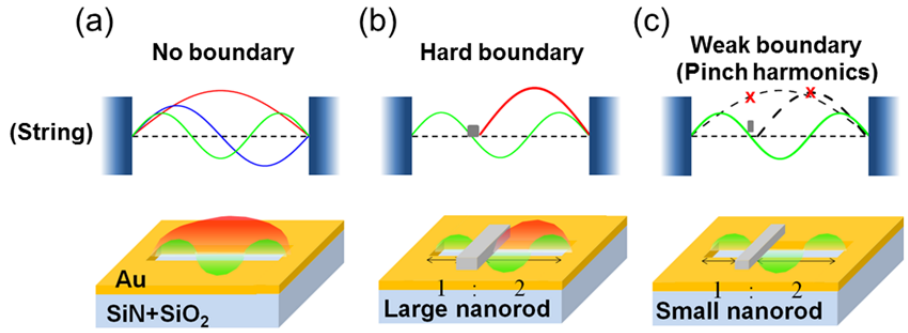

Figure 6.2 Schematics of standing waves (n=1, 2, and 3) on a string without touch (a), two isolated fundamental modes on each side by a finger located at 1:2 position (b), and dominant third harmonic mode by a pinch harmonic technique (c). In the bottom, schematic diagrams of THz nano-slot antennas without nanorod (a), with a large nanorod (b), and with a smaller nanorod (c) at 1:2 position on the hole.

6.2 Experimental results

Shown in Fig. 6.3 are transmission spectra of vertically-aligned single nano-slot antennas in the frequency range from 0.1 THz to 1.1 THz using THz time domain spectroscopy.[20,81] The THz nano-slot antennas, patterned by focused ion beam (FIB), have dimensions of l_1=300 μm and w_1=120 nm on gold film of 60 nm thickness deposited onto a 2 μm-thick SiN/SiO_2 substrate, inducing strong electric field enhancement of more than 1,000 inside the aperture at the fundamental resonance of 0.26 THz. We prepare two nanorods (Fig. 6.1(b) (bottom)) by Pt-deposition method using FIB. The larger rod (Fig. 6.1(b), bottom left) has a dimension of l_2=1 μm, w_2=600 nm, and t_2=400 nm, while the smaller one (Fig. 6.1(b), bottom right) has l_2=1 μm, w_2=250 nm, and

t_2=250 nm. When we put the larger nanorod at the 1:2 position, the resonance peak is pushed to about 0.34 THz caused by the new nano-slot antenna with the length of 200 μm. For the smaller nanorod placed at 1:2 position, indeed the third harmonic resonance (f_{res}=0.78 THz) dominates in the pinch harmonic sense. Despite this dominance, the original fundamental mode still peaks with a high frequency shoulder mostly likely from the fundamental mode of the long side.

When we move the small nanorod to the 1:1 position, the symmetry of the system brings further profound change to the transmission spectra. Putting the nanorod to the mid-point turns off the n=1, 3, 5 modes. Even the n=2 mode, which can survive because it has node in the middle, do not radiate to the far-field because the positive and negative parts cancel: $E_{far} = \frac{e^{ikR}}{i\lambda R}\int E_{near} dA$ according to Kirchhoff formalism, where R is the distance from the aperture to the detector and A is the aperture area.[82] Figure 6.3(b) shows transmittance spectra, measured for the same l_1=300 μm nano-slot antennas without nanorods, and with the same parameter small nanorod as used in Fig. 6.3(a). The fundamental and third harmonic modes are almost completely suppressed.

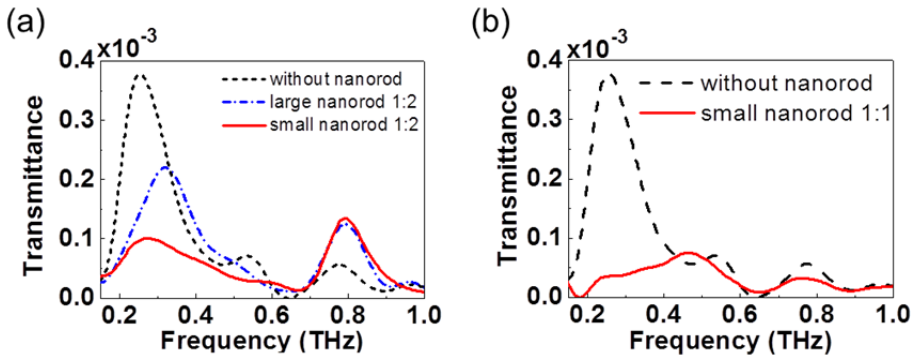

Figure 6.3 (a) Experimental transmittance through single THz nano-slot antennas with the single larger (600 nm-wide) and smaller (250 nm-wide) metallic nanorods at the 1:2 position, and without nanorod. (b) Transmittance spectra through the same nano-slot antennas without nanorod and with the same parameter small nanorod, as shown in (a), at 1:1 position

6.3 Theoretical calculations: Microscopic diffraction model

For better insight into THz pinch harmonics, a microscopic diffraction model with a gold nanorod fit into the slot is carried out, as shown in Fig. 6.4(a) (top). In a view of microscopic diffraction of light,[80] we consider the simplified model as in Fig. 6.4(a) (bottom) fitting the nanorod with a width *s* at the location of P_2. When light passes through a long rectangular aperture at the normal incidence, resonance of light inside the slot arises due to the constructive build-up of reflected components of electromagnetic waves by the edge of rectangle. When the nanorod is placed inside the aperture, it causes partial reflection and transmission of light. The partially transmitted light gets reflected at the other edge (P3) and destructively interferes with the reflected light by nanorod, resulting in THz pinch harmonics.

We assume that scattered light with electric field amplitude E_1^0 is injected at P_1. Then the subsequent electric field inside the rectangle with the length d_1+d_2 due to the multiple reflections is described by

$$E_{region1}(d_1,d_2) = E_1 e^{ikx} + E_2 e^{ik(d_1-x)}, \qquad 0 \le x \le d_1$$
$$E_{region2}(d_1,d_2) = E_3 e^{ik(x-d_1)} + E_4 e^{ik(d_1+d_2-x)}, \qquad d_1 \le x \le d_1+d_2$$
$$E(d_1,d_2) = E_{region1}(d_1,d_2) + E_{region2}(d_1,d_2)$$

If we denote E_1^m to be the amplitude of light injected at P_1 after m-times reflection, we find that

$$E_1 = E_1^0 + E_1^1 + \cdots = \frac{E_1^0}{1-\eta}, \text{ where } \eta = e^{i2kd_1}\left(\beta r + \frac{t^2 r^2 e^{i2kd_2}}{1-\beta r e^{i2kd_2}}\right)$$
$$E_2 = E_1 e^{ikd_1}\left(\beta + \frac{t^2 r e^{i2kd_2}}{1-\beta r e^{i2kd_2}}\right), \quad E_3 = \frac{E_1 t e^{ikd_1}}{1-\beta r e^{i2kd_2}}, \quad E_4 = \frac{E_1 t r e^{ik(d_1+d_2)}}{1-\beta r e^{i2kd_2}},$$

where $t = e^{-\frac{s}{\delta}}$ is the transmission coefficient through the nanorod with the width *s*, δ the skin depth of gold, $\beta = -\sqrt{1-t^2}$ the reflection coefficient at the nanorod, and *r* the reflection coefficient at two edges. Since light is also injected via diffraction at the other edge P_3, the total electric field is given by $E_{tot} = E(d_1,d_2) + E(d_2,d_1)$. Diffractions at the nanorod with sub-skindepth dimensions can be ignored.[14,16,83,84] The magnitude of transmission resonance, in the Kirchhoff sense, is given by $\int_0^{d_1+d_2} E_{tot}\,dx$.

Figure 6.4(b) and 6.4(c) shows transmitted spectra with the nanorods at the 1:2 and 1:1 positions obtained from our microscopic diffraction model. At an *s* of around 0.3δ, we obtain qualitatively similar results with the experiments shown in Fig. 6.3. However, the dimension of the nanorod in experiments is about two times larger than its skin depth. This difference is because the coupled electromagnetic wave could feel the nanorod with bridge-type geometry as a thinner partition than its original size.

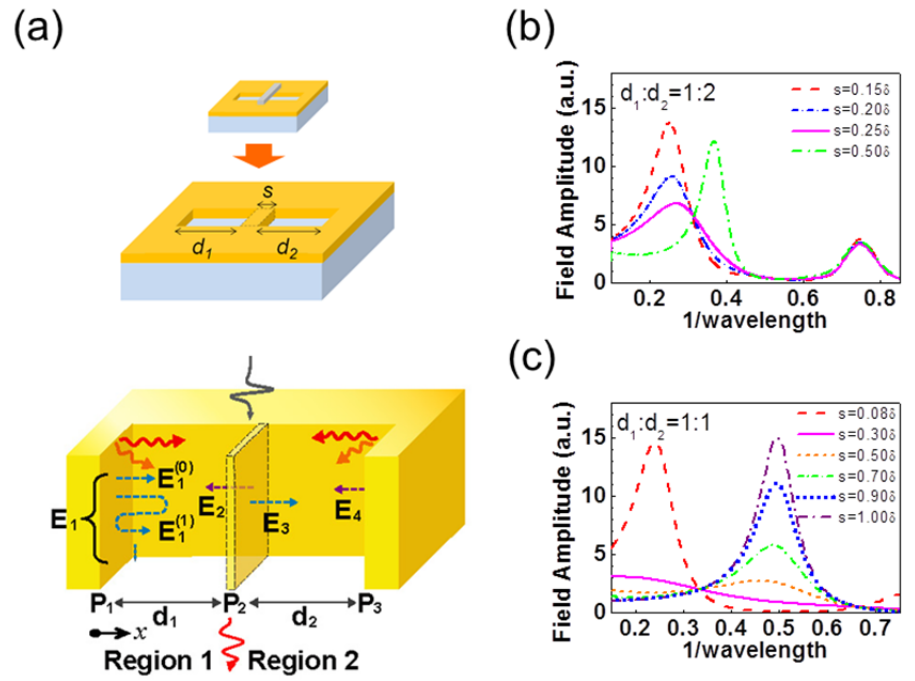

Figure 6.4 (a) (Top) Schematic diagram of a simplified model with a gold nanorod (width *s*) at d_1:d_2 position inside the THz nano-slot antenna. (Bottom) Microscopic diffraction processes at the nanorod and the two edges of the aperture under illumination by the THz wave at the normal incidence. (b) Transmitted field amplitude spectra of the samples with various nanorod widths at 1:2 position inside the slot, obtained by the microscopic diffraction theory. (c) The same as (b) except the 1:1 position.

6.4 Conclusions

We present a new THz metamaterial shifting its resonance to the higher harmonic by a single nanorod on each THz nano-slot antenna, depending on the rod-size and rod-position, analogous to the pinch harmonics. Unlike pinch harmonics by guitar, the nanorod at 1:1 position on the aperture strikingly shuts off all the resonance up to 80%, showing a novel aspect of THz pinch

harmonics. It has a great potential for developing applications to block the strongly funnelled electric fields inside hundreds micron length holes by relatively small nano-sized particle. This ability might prove crucial in achieving terahertz electrical or optical switching devices[40,85], detecting nanoparticles,[86-90] and developing new applications using nanorods or nanowires.[91,92]

Chapter 7 Detection of single nano-particle embedded in terahertz nano-slot antenna

7.1 Introduction

Observation of single nanoparticles, having dimensions in deep sub-wavelength region, has been still a big issue since it requires detection of very weak light absorption or scattering. Recently, the ability to detect individual nanoparticles using sub-wavelength metallic structures, such as plasmonic dipole antennas and microresonator, has been a widely spread tool for observing optical properties of single metallic nanoparticles and biomolecules.[33,34,71,93,94] Here, we investigate whether single metallic nanoparticles with a dimension of 100 nm fitted into nano-slot can be detected using a THz wave with sub-millimeter wavelength. Strikingly, single gold nanoparticles inside single THz nano-slot antenna induce a noticeable modulation of the THz transmission through the slot. This ability would pave a new way for detecting nanoparticles in infrared and THz regimes.

7.2 Absorption and scattering cross section of gold nanoparticle

According to Optical theorem introduced by Sellmeier and Rayleigh, absorption and scattering cross section (C_{abs} and C_{sca}) of small particles are the following:[95]

$$C_{abs} = \frac{2\pi}{\lambda}\mathrm{Im}[\alpha] = k\,\mathrm{Im}[\alpha] \text{ and } C_{sca} = \frac{k^4}{6\pi}|\alpha|^2 = \frac{1}{6\pi}\left(\frac{2\pi}{\lambda}\right)^4|\alpha|^2$$

where α is the polarizability of the particle. The polarizability α of the spherical metallic particle surrounded by vacuum is

$$\alpha = 4\pi a^3\frac{\varepsilon - 1}{\varepsilon + 2} = 3V\frac{\varepsilon - 1}{\varepsilon + 2}$$

where ε the dielectric constant of the metal, V the volume of the particle, and a the radius of the sphere.

When we consider one gold nanoparticle with a diameter of 100 nm at the wavelength of 500 μm, the absorption and scattering cross section of this gold nanoparticle in free space are the following:

$$C_{abs} = 9.30\times10^{-23}\,\mathrm{m}^2 \text{ and } C_{sca} = 3.26\times10^{-27}\,\mathrm{m}^2$$

In THz experiments, the area of incident THz wave is 10^{-6} m^2 and the signal to noise ratio of our THz transmission setup is about 10^4. The detection limitation of our experimental setup is about 10^{-10} m^2. Therefore, when a single gold nanoparticle exists in free space, it would be so difficult to see the THz transmission modulation enabled by the particle because the absorption cross section of the particle is much smaller than the detection limitation of our experimental setup. For overcoming the diffraction limit, we suggest THz nano-slot antenna as a new tool for the detection of a single gold nanoparticle inside the slot in the THz region.

7.3 Experimental results

In this section, we experimentally demonstrate THz transmission modulation enabled by placing a single gold nanoparticle inside a single THz nano-slot antenna (Fig. 7.1(a)). When we put gold nanoparticles with the diameter of 100 nm into the THz nano-slot antenna with the length of 150 μm and the width of 120 nm, as shown in Fig 7.1 (b) and (c), the nanoparticle as an obstacle could disturb the fundamental resonant mode in the hundreds of micrometer length hole despite the particle's dimension being smaller than about $\frac{\lambda}{5{,}000}$.[18]

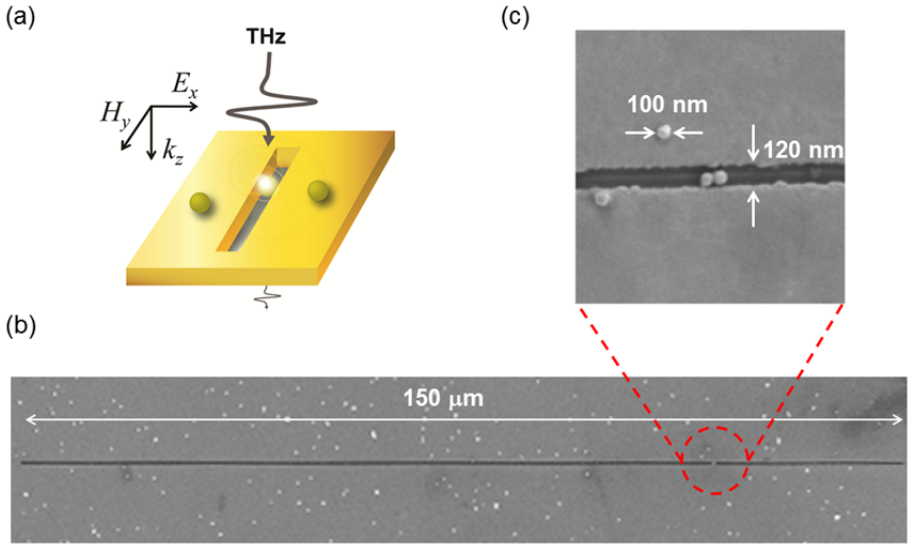

Figure 7.1 (a) Schematic of a single gold nanoparticle inside a single THz nano-slot antenna. Only the nanoparticle inside the slot antenna can be strongly coupled with a terahertz wave. (b) Scanning electron microscopy (SEM) image of the THz nano-slot antenna with a length of 150 mm and a

width of 120 nm on a 100 nm-thick gold film. (c) Enlarged SEM image of only two single gold nanoparticles with a diameter of 100 nm inside the slot

Figure 7.2(a) depicts the schematic diagram of the sample fabrication process using the method of drop-drying the gold nanoparticles solution onto the slot sample.[87,96] When we put just two gold nanoparticles inside the THz nano-slot antenna, as shown in Fig. 7.2(b), the resonant transmission amplitude is decreased to 65 % in Fig. 7.2(d). When we put 2 times more nanoparticles of 1.1×10^{8} inside the slot, the resonant transmission becomes totally blocked. For the control experiment on bare quartz substrate without the metallic pattern, we put 40 times more same nanoparticles onto the bare quartz, as shown in Fig. 7.2(c). In Fig. 7.2(e), as increasing the number of the particles until 1.3×10^{9}, the THz transmission maintains almost 1 because the total absorption cross section of the 100 nm gold nanoparticles, 10^{-13} m^2, is much smaller than the area needed for the detection using our THz experimental setup, 10^{-10} m^2. To observe noticeable transmission modulation by the nanoparticles without the slot antenna, we need 1,000 times more nanoparticles of about 1.08×10^{12} on the bare substrate than the largest number of the particles when we used the slot antenna. This phenomenon is attributed to the presence of the strong local field, which could increase the scattering or the absorption from particles thereby enabling detection of subwavelength particles beyond the diffraction limit.[97]

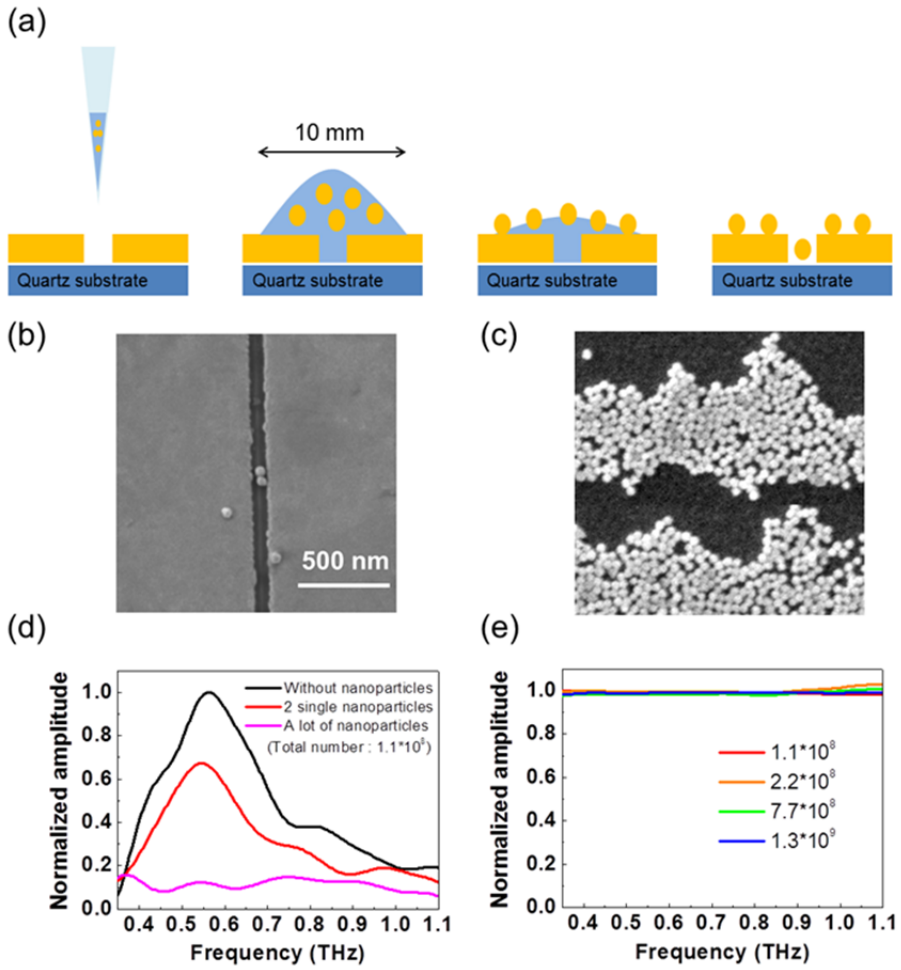

Figure 7.2 (a) Schematic diagram of the process during the early stages of drying the solution with the gold nanoparticles (not to scale), showing how nanoparticles are located inside the THz slot antenna. (b) Enlarged SEM image of only two single gold nanoparticles with a size of 100 nm inside the slot. Other $5.5*10^7$ nanoparticles outside the slot are located in the circular area with a diameter of 10 mm around the THz slot antenna (Density: 1.7 μm^{-2}). (c) Enlarged SEM image of a lot of same gold nanoparticles with total number of $1.3*10^9$ in the same area on the bare quartz substrate. (d) Experimental normalized transmitted (electric field) amplitude spectra

through a single THz nano-slot antenna without and with gold nanoparticles. (e) Normalized amplitude spectra through the same gold nanoparticles with the density of 41 μm^{-2} on the bare quartz substrate, using transmitted amplitude through the bare quartz without nanoparticles as a reference

7.4 Conclusions

In summary, we have successfully detected 100 nm single gold nanoparticles using the single THz nano-slot antenna. Single gold nanoparticle fitted into the nano-slot induces the dramatic changes in the amplitude of the resonant transmission up to 35 %. This modulation is accompanied by the strong coupling between the gold nanoparticles and the slot antenna, disturbing the fundamental resonant mode of the slot antenna. This work unveils the potential associated to nanoparticles detection in far-infrared and THz frequency regions with localized surface plasmon resonance based sensing techniques, in order to observe sensitively organic or bio molecules, having the absorption resonances enabled by their vibrational modes in the millimeter wavelength region.

Chapter 8 Conclusions

In this thesis, the coupling effects between THz nano-slot antenna and metallic nano-objects, such as, nano-barrier, nano-rod, and nano-particle, has been investigated both experimentally and theoretically at the slot antenna's resonance. We have also introduced standard fabrication procedures, such as focused ion beam and electron-beam lithography, for providing a general recipe for the implementation of the rectangular hole with hundreds micron length and nano-sized width, acting as a slot antenna in THz region. These nano-slot antenna samples are observed by the transmission-type THz time-domain spectroscopy with high signal-to-noise ratio of over 10000:1 and tightly focused spot size of below 1 mm.

The first part of this thesis deals with detailed fundamental investigations of the THz nano-slot antennas. We have demonstrated that the strong electric field enhancement of the single nano-slot with the width of about 100 nm is over 1000 at its resonance. We have also shown that an ultra-broadband performance with average normalized amplitude of 70 % can be realized through log-periodic THz slot antennas with a striking aspect ratio of 400:1 and large field enhancement in THz region. It should be noted that nano-slot antennas have the decisive advantage over microns wide structures in that the lateral distances between two adjacent slots can be very small, to be less than 5 μm. This ability to close-packing many antennas within small area, still maintaining a small coverage, is crucial in achieving the broad spectrum and high transmittance without sacrificing large field enhancement.

Moreover, we have showed vertical coupling between two nano-slot antennas separated by a single metallic nano-barrier. The proposed system has enabled

the observation of the transition state arising at the continuous crossover between the half- and the full-wavelength states supported by the slot antenna. This work opens new potentials to tailor the control of terahertz electromagnetic wave using deep sub-skin metallic nano-objects and may lead to the realization of novel schemes for ultrasensitive tuning and detection of nanoscale objects using electromagnetic wave with a millimeter wavelength.

Finally, we have proposed a new concept in strong coupling between the nano-slot antenna and metallic nanoparticles. We showed that a single gold nanoparticle placed on or fitted into THz nano-slot antenna greatly influences its spectrum, shifting one specific resonance analogous to pinch harmonics, or decreasing the amplitude of the resonant transmission. This ability provides new physical origin for controlling far-field transmission without the need to change dielectric property of the whole substrate under the slot[22,40], which limits speed. Moreover, the extreme sensitivity to nanoparticle dimensions and positions promises a new scheme for nanoparticle detection.

Bibilography

[1] T. W. Ebbesen, H. J. Lezec, H. F. Ghaemi, T. Thio, and P. A. Wolff, "Extraordinary optical transmission through sub-wavelength hole arrays", Nature **391**, 667 (1998).

[2] D. R. Smith, J. B. Pendry, and M. C. K. Wiltshire, "Metamaterials and negative refractive index", Science **305**, 788 (2004).

[3] J. B. Pendry, L. Martin-Moreno, and F. J. Garcia-Vidal, "Mimicking surface plasmons with structured surfaces", Science **305**, 847 (2004).

[4] T. Tanemura, K. C. Balram, D. S. Ly-Gagnon, P. Wahl, J. S. White, M. L. Brongersma, and D. A. B. Miller, "Multiple-Wavelength Focusing of Surface Plasmons with a Nonperiodic Nanoslit Coupler", Nano Lett. **11**, 2693 (2011).

[5] F. J. Garcia-Vidal, E. Moreno, J. A. Porto, and L. Martin-Moreno, "Transmission of light through a single rectangular hole", Phys. Rev. Lett. **95**, 103901 (2005).

[6] F. J. Garcia-Vidal, L. Martin-Moreno, T. W. Ebbesen, and L. Kuipers, "Light passing through subwavelength apertures", Rev. Mod. Phys. **82**, 729 (2010).

[7] M. A. Seo, A. J. L. Adam, J. H. Kang, J. W. Lee, K. J. Ahn, Q. H. Park, P. C. M. Planken, and D. S. Kim, "Near field imaging of terahertz focusing onto rectangular apertures", Opt. Express **16**, 20484 (2008).

[8] M. A. Seo, H. R. Park, D. J. Park, D. Kim, A. J. L. Adam, and P. C. M.

Planken, "Focusing of Terahertz Waves onto Micron-sized Slits Grown on ZnTe and GaP Substrates", J Korean Phys Soc **55**, 267 (2009).

[9] F. Keilmann, "Infrared High-Pass Filter with High Contrast", Int J Infrared Milli **2**, 259 (1981).

[10] K. J. K. Koerkamp, S. Enoch, F. B. Segerink, N. F. van Hulst, and L. Kuipers, "Strong influence of hole shape on extraordinary transmission through periodic arrays of subwavelength holes", Phys. Rev. Lett. **92**, (2004).

[11] K. L. van der Molen, K. J. Klein Koerkamp, S. Enoch, F. B. Segerink, N. F. van Hulst, and L. Kuipers, "Role of shape and localized resonances in extraordinary transmission through periodic arrays of subwavelength holes: Experiment and theory", Phys. Rev. B **72**, (2005).

[12] H. Cao and A. Nahata, "Influence of aperture shape on the transmission properties of a periodic array of subwavelength apertures", Opt. Express **12**, 3664 (2004).

[13] H. R. Park, Y. M. Park, H. S. Kim, J. S. Kyoung, M. A. Seo, D. J. Park, Y. H. Ahn, K. J. Ahn, and D. S. Kim, "Terahertz nanoresonators: Giant field enhancement and ultrabroadband performance", Appl. Phys. Lett. **96**, 121106 (2010).

[14] A. K. Azad and W. L. Zhang, "Resonant terahertz transmission in subwavelength metallic hole arrays of sub-skin-depth thickness", Opt.

Lett. **30**, 2945 (2005).

[15] X. Shou, A. Agrawal, and A. Nahata, "Role of metal film thickness on the enhanced transmission properties of a periodic array of subwavelength apertures", Opt. Express **13**, 9834 (2005).

[16] R. Singh, E. Smirnova, A. J. Taylor, J. F. O'Hara, and W. L. Zhang, "Optically thin terahertz metamaterials", Opt. Express **16**, 6537 (2008).

[17] H. C. Guo, T. P. Meyrath, T. Zentgraf, N. Liu, L. W. Fu, H. Schweizer, and H. Giessen, "Optical resonances of bowtie slot antennas and their geometry and material dependence", Opt. Express **16**, 7756 (2008).

[18] H. R. Park, Y. M. Bahk, J. H. Choe, S. Han, S. S. Choi, K. J. Ahn, N. Park, Q. H. Park, and D. S. Kim, "Terahertz pinch harmonics enabled by single nano rods", Opt Express **19**, 24775 (2011).

[19] L. A. Giannuzzi and F. A. Stevie, "A review of focused ion beam milling techniques for TEM specimen preparation", Micron **30**, 197 (1999).

[20] M. Seo, J. Kyoung, H. Park, S. Koo, H. S. Kim, H. Bernien, B. J. Kim, J. H. Choe, Y. H. Ahn, H. T. Kim, N. Park, Q. H. Park, K. Ahn, and D. S. Kim, "Active Terahertz Nanoantennas Based on VO(2) Phase Transition", Nano Lett **10**, 2064 (2010).

[21] Y. G. Jeong, H. Bernien, J. S. Kyoung, H. R. Park, H. S. Kim, J. W. Choi, B. J. Kim, H. T. Kim, K. J. Ahn, and D. S. Kim, "Electrical control of terahertz nano antennas on VO2 thin film", Opt. Express **19**,

21211 (2011).

[22] J. Kyoung, M. Seo, H. Park, S. Koo, H. S. Kim, Y. Park, B. J. Kim, K. Ahn, N. Park, H. T. Kim, and D. S. Kim, "Giant nonlinear response of terahertz nanoresonators on VO2 thin film", Opt. Express **18**, 16452 (2010).

[23] S. B. Choi, J. S. Kyoung, H. S. Kim, H. R. Park, D. J. Park, B. J. Kim, Y. H. Ahn, F. Rotermund, H. T. Kim, K. J. Ahn, and D. S. Kim, "Nanopattern enabled terahertz all-optical switching on vanadium dioxide thin film", Appl. Phys. Lett. **98**, (2011).

[24] M. Vanexter, C. Fattinger, and D. Grischkowsky, "Terahertz Time-Domain Spectroscopy of Water-Vapor", Opt. Lett. **14**, 1128 (1989).

[25] Q. Wu, M. Litz, and X. C. Zhang, "Broadband detection capability of ZnTe electro-optic field detectors", Appl. Phys. Lett. **68**, 2924 (1996).

[26] M. A. Seo, H. R. Park, S. M. Koo, D. J. Park, J. H. Kang, O. K. Suwal, S. S. Choi, P. C. M. Planken, G. S. Park, N. K. Park, Q. H. Park, and D. S. Kim, "Terahertz field enhancement by a metallic nano slit operating beyond the skin-depth limit", Nat. Photonics **3**, 152 (2009).

[27] G. Klatt, B. Surrer, D. Stephan, O. Schubert, M. Fischer, J. Faist, A. Leitenstorfer, R. Huber, and T. Dekorsy, "Photo-Dember terahertz emitter excited with an Er:fiber laser", Appl. Phys. Lett. **98**, (2011).

[28] D. J. Park, S. B. Choi, Y. H. Ahn, F. Rotermund, I. B. Sohn, C. Kang, M. S. Jeong, and D. S. Kim, "Terahertz near-field enhancement in narrow rectangular apertures on metal film", Opt. Express **17**, 12493

(2009).

[29] F. Miyamaru and M. Hangyo, "Strong enhancement of terahertz transmission for a three-layer heterostructure of metal hole arrays", Physical Review B **72**, 035429 (2005).

[30] H. R. Park, Y. M. Bahk, K. J. Ahn, Q. H. Park, D. S. Kim, L. Martin-Moreno, F. J. Garcia-Vidal, and J. Bravo-Abad, "Controlling Terahertz Radiation with Nanoscale Metal Barriers Embedded in Nano Slot Antennas", Acs Nano **5**, 8340 (2011).

[31] J. H. Kang, J. H. Choe, D. S. Kim, and Q. H. Park, "Substrate effect on aperture resonances in a thin metal film", Opt. Express **17**, 15652 (2009).

[32] H. R. Park, S. M. Koo, O. K. Suwal, Y. M. Park, J. S. Kyoung, M. A. Seo, S. S. Choi, N. K. Park, D. S. Kim, and K. J. Ahn, "Resonance behavior of single ultrathin slot antennas on finite dielectric substrates in terahertz regime", Appl. Phys. Lett. **96**, 211109 (2010).

[33] K. Lindfors, T. Kalkbrenner, P. Stoller, and V. Sandoghdar, "Detection and spectroscopy of gold nanoparticles using supercontinuum white light confocal microscopy", Phys. Rev. Lett. **93**, 037401 (2004).

[34] J. G. Zhu, S. K. Ozdemir, Y. F. Xiao, L. Li, L. N. He, D. R. Chen, and L. Yang, "On-chip single nanoparticle detection and sizing by mode splitting in an ultrahigh-Q microresonator (vol 4, pg 46, 2010)", Nat. Photonics **4**, 122 (2010).

[35] M. X. Ren, B. H. Jia, J. Y. Ou, E. Plum, J. F. Zhang, K. F. MacDonald,

A. E. Nikolaenko, J. J. Xu, M. Gu, and N. I. Zheludev, "Nanostructured Plasmonic Medium for Terahertz Bandwidth All-Optical Switching", Adv Mater **23**, 5540 (2011).

[36] E. A. Zibik, T. Grange, B. A. Carpenter, N. E. Porter, R. Ferreira, G. Bastard, D. Stehr, S. Winnerl, M. Helm, H. Y. Liu, M. S. Skolnick, and L. R. Wilson, "Long lifetimes of quantum-dot intersublevel transitions in the terahertz range", Nat. Mater. **8**, 803 (2009).

[37] M. Wagner, H. Schneider, D. Stehr, S. Winnerl, A. M. Andrews, S. Schartner, G. Strasser, and M. Helm, "Terahertz nonlinear optics using intra-excitonic quantum well transitions: Sideband generation and AC Stark splitting", Physica Status Solidi B-Basic Solid State Physics **248**, 859 (2011).

[38] M. C. Hoffmann, J. Hebling, H. Y. Hwang, K. L. Yeh, and K. A. Nelson, "Impact ionization in InSb probed by terahertz pump-terahertz probe spectroscopy", Phys. Rev. B **79**, (2009).

[39] H. T. Chen, W. J. Padilla, M. J. Cich, A. K. Azad, R. D. Averitt, and A. J. Taylor, "A metamaterial solid-state terahertz phase modulator", Nat. Photonics **3**, 148 (2009).

[40] H. T. Chen, W. J. Padilla, J. M. O. Zide, A. C. Gossard, A. J. Taylor, and R. D. Averitt, "Active terahertz metamaterial devices", Nature **444**, 597 (2006).

[41] J. W. Lee, M. A. Seo, D. H. Kang, K. S. Khim, S. C. Jeoung, and D. S. Kim, "Terahertz electromagnetic wave transmission through random

arrays of single rectangular holes and slits in thin metallic sheets", Phys. Rev. Lett. **99**, 137401 (2007).

[42] J. W. Lee, M. A. Seo, D. J. Park, D. S. Kim, S. C. Jeoung, C. Lienau, Q. H. Park, and P. C. M. Planken, "Shape resonance omni-directional terahertz filters with near-unity transmittance", Opt. Express **14**, 1253 (2006).

[43] J. W. Lee, M. A. Seo, D. S. Kim, S. C. Jeoung, C. Lienau, J. H. Kang, and Q. H. Park, "Fabry-Perot effects in THz time-domain spectroscopy of plasmonic band-gap structures", Appl. Phys. Lett. **88**, 071114 (2006).

[44] H. Lochbihler and R. Depine, "Highly Conducting Wire Gratings in the Resonance Region", Applied Optics **32**, 3459 (1993).

[45] D. J. Park, S. B. Choi, Y. H. Ahn, Q. H. Park, and D. S. Kim, "Theoretical Study of Terahertz Near-Field Enhancement Assisted by Shape Resonance in Rectangular Hole Arrays in Metal Films", J. Korean Phys. Soc. **54**, 64 (2009).

[46] A. I. Fernandez-Dominguez, F. J. Garcia-Vidal, and L. Martin-Moreno, "Resonant transmission of light through finite arrays of slits", Phys. Rev. B **76**, 235430 (2007).

[47] D. Pacifici, H. J. Lezec, H. A. Atwater, and J. Weiner, "Quantitative determination of optical transmission through subwavelength slit arrays in Ag films: Role of surface wave interference and local coupling between adjacent slits", Phys. Rev. B **77**, 115411 (2008).

[48] J. G. Han, J. Q. Gu, X. C. Lu, M. X. He, Q. R. Xing, and W. L. Zhang, "Broadband resonant terahertz transmission in a composite metal-dielectric structure", Opt. Express **17**, 16527 (2009).

[49] R. H. Duhamel and D. E. Isbell, "Broadband Logarithmically Periodic Antenna Structures", P. IRE **45**, 385 (1957).

[50] C. A. Balanis, *Antenna Theory* (John Wiley & Sons Inc Hoboken, New Jersey, 2005).

[51] T. Driscoll, H. T. Kim, B. G. Chae, B. J. Kim, Y. W. Lee, N. M. Jokerst, S. Palit, D. R. Smith, M. Di Ventra, and D. N. Basov, "Memory Metamaterials", Science **325**, 1518 (2009).

[52] T. J. Yen, W. J. Padilla, N. Fang, D. C. Vier, D. R. Smith, J. B. Pendry, D. N. Basov, and X. Zhang, "Terahertz magnetic response from artificial materials", Science **303**, 1494 (2004).

[53] D. S. Kim, S. C. Hohng, V. Malyarchuk, Y. C. Yoon, Y. H. Ahn, K. J. Yee, J. W. Park, J. Kim, Q. H. Park, and C. Lienau, "Microscopic origin of surface-plasmon radiation in plasmonic band-gap nanostructures", Phys. Rev. Lett. **91**, 143901 (2003).

[54] J. Bravo-Abad, L. Martin-Moreno, and F. J. Garcia-Vidal, "Resonant transmission of light through subwavelength holes in thick metal films", Ieee J Sel Top Quant **12**, 1221 (2006).

[55] F. J. Garcia-Vidal, L. Martin-Moreno, E. Moreno, L. K. S. Kumar, and R. Gordon, "Transmission of light through a single rectangular hole in a real metal", Phys. Rev. B **74**, 153411 (2006).

[56] A. Degiron, H. J. Lezec, N. Yamamoto, and T. W. Ebbesen, "Optical transmission properties of a single subwavelength aperture in a real metal", Opt. Commun. **239**, 61 (2004).

[57] N. Liu, L. Langguth, T. Weiss, J. Kastel, M. Fleischhauer, T. Pfau, and H. Giessen, "Plasmonic analogue of electromagnetically induced transparency at the Drude damping limit", Nat. Mater. **8**, 758 (2009).

[58] B. Feng, Z. X. Li, and X. Zhang, "Effect of grain-boundary scattering on the thermal conductivity of nanocrystalline metallic films", J Phys D Appl Phys **42**, 055311 (2009).

[59] S. Zhang, W. J. Fan, K. J. Malloy, S. R. J. Brueck, N. C. Panoiu, and R. O. Osgood, "Demonstration of metal-dielectric negative-index metamaterials with improved performance at optical frequencies", J Opt Soc Am B **23**, 434 (2006).

[60] Y. M. Bahk, H. R. Park, K. J. Ahn, H. S. Kim, Y. H. Ahn, D. S. Kim, J. Bravo-Abad, L. Martin-Moreno, and F. J. Garcia-Vidal, "Anomalous Band Formation in Arrays of Terahertz Nanoresonators", Phys. Rev. Lett. **106**, 013902 (2011).

[61] L. R. Hirsch, R. J. Stafford, J. A. Bankson, S. R. Sershen, B. Rivera, R. E. Price, J. D. Hazle, N. J. Halas, and J. L. West, "Nanoshell-mediated near-infrared thermal therapy of tumors under magnetic resonance guidance", P Natl Acad Sci USA **100**, 13549 (2003).

[62] E. Prodan, C. Radloff, N. J. Halas, and P. Nordlander, "A hybridization model for the plasmon response of complex

nanostructures", Science **302**, 419 (2003).

[63] C. Loo, A. Lin, L. Hirsch, M. H. Lee, J. Barton, N. J. Halas, J. West, and R. Drezek, "Nanoshell-enabled photonics-based imaging and therapy of cancer", Technol Cancer Res T **3**, 33 (2004).

[64] P. Muhlschlegel, H. J. Eisler, O. J. F. Martin, B. Hecht, and D. W. Pohl, "Resonant optical antennas", Science **308**, 1607 (2005).

[65] J. A. Schuller, E. S. Barnard, W. S. Cai, Y. C. Jun, J. S. White, and M. L. Brongersma, "Plasmonics for extreme light concentration and manipulation", Nat. Mater. **9**, 193 (2010).

[66] B. Ogut, R. Vogelgesang, W. Sigle, N. Talebi, C. T. Koch, and P. A. van Aken, "Hybridized Metal Slit Eigenmodes as an Illustration of Babinet's Principle", Acs Nano **5**, 6701 (2011).

[67] Z. H. Kim, D. S. Kim, J. Heo, S. H. Ahn, S. W. Han, and W. S. Yun, "Real-Space Mapping of the Strongly Coupled Plasmons of Nanoparticle Dimers", Nano Lett. **9**, 3619 (2009).

[68] T. Atay, J. H. Song, and A. V. Nurmikko, "Strongly interacting plasmon nanoparticle pairs: From dipole-dipole interaction to conductively coupled regime", Nano Lett. **4**, 1627 (2004).

[69] D. P. Fromm, A. Sundaramurthy, P. J. Schuck, G. Kino, and W. E. Moerner, "Gap-dependent optical coupling of single "Bowtie" nanoantennas resonant in the visible", Nano Lett. **4**, 957 (2004).

[70] R. Hillenbrand, M. Schnell, A. Garcia-Etxarri, J. Alkorta, and J. Aizpurua, "Phase-Resolved Mapping of the Near-Field Vector and

Polarization State in Nanoscale Antenna Gaps", Nano Lett. **10**, 3524 (2010).

[71] M. Righini, P. Ghenuche, S. Cherukulappurath, V. Myroshnychenko, F. J. G. de Abajo, and R. Quidant, "Nano-optical Trapping of Rayleigh Particles and Escherichia coli Bacteria with Resonant Optical Antennas", Nano Lett. **9**, 3387 (2009).

[72] S. Arnold, D. Keng, S. I. Shopova, S. Holler, W. Zurawsky, and F. Vollmer, "Whispering gallery mode carousel - a photonic mechanism for enhanced nanoparticle detection in biosensing", Opt. Express **17**, 6230 (2009).

[73] M. Schnell, A. Garcia-Etxarri, A. J. Huber, K. Crozier, J. Aizpurua, and R. Hillenbrand, "Controlling the near-field oscillations of loaded plasmonic nanoantennas", Nat. Photonics **3**, 287 (2009).

[74] A. Alu and N. Engheta, "Tuning the scattering response of optical nanoantennas with nanocircuit loads", Nat. Photonics **2**, 307 (2008).

[75] N. J. Halas, J. B. Lassiter, J. Aizpurua, L. I. Hernandez, D. W. Brandl, I. Romero, S. Lal, J. H. Hafner, and P. Nordlander, "Close encounters between two nanoshells", Nano Lett. **8**, 1212 (2008).

[76] M. Danckwerts and L. Novotny, "Optical frequency mixing at coupled gold nanoparticles", Phys. Rev. Lett. **98**, 026104 (2007).

[77] J. Zuloaga, E. Prodan, and P. Nordlander, "Quantum Description of the Plasmon Resonances of a Nanoparticle Dimer", Nano Lett. **9**, 887 (2009).

[78] M. A. Ordal, L. L. Long, R. J. Bell, S. E. Bell, R. R. Bell, R. W. Alexander, and C. A. Ward, "Optical-Properties of the Metals Al, Co, Cu, Au, Fe, Pb, Ni, Pd, Pt, Ag, Ti, and W in the Infrared and Far Infrared", Appl. Optics **22**, 1099 (1983).

[79] M. Davis, "Guitar strings as standing waves: A demonstration", J. Chem. Educ. **84**, 1287 (2007).

[80] H. T. Liu and P. Lalanne, "Microscopic theory of the extraordinary optical transmission", Nature **452**, 728 (2008).

[81] M. Van exter, C. Fattinger, and D. Grischkowsky, "Terahertz Time-Domain Spectroscopy of Water-Vapor", Opt. Lett. **14**, 1128 (1989).

[82] J. S. Kyoung, M. A. Seo, H. R. Park, K. J. Ahn, and D. S. Kim, "Far field detection of terahertz near field enhancement of sub-wavelength slits using Kirchhoff integral formalism", Opt. Commun. **283**, 4907 (2010).

[83] S. Koo, M. S. Kumar, J. Shin, D. Kim, and N. Park, "Extraordinary Magnetic Field Enhancement with Metallic Nanowire: Role of Surface Impedance in Babinet's Principle for Sub-Skin-Depth Regime", Phys. Rev. Lett. **103**, 263901 (2009).

[84] R. Marques, F. Mesa, J. Martel, and F. Medina, "Comparative analysis of edge- and broadside-coupled split ring resonators for metamaterial design - Theory and experiments", Ieee T. Antenn. Propag. **51**, 2572 (2003).

[85] K. F. MacDonald, Z. L. Samson, M. I. Stockman, and N. I. Zheludev,

"Ultrafast active plasmonics", Nat. Photonics **3**, 55 (2009).

[86] V. Juve, A. Crut, P. Maioli, M. Pellarin, M. Broyer, N. Del Fatti, and F. Vallee, "Probing Elasticity at the Nanoscale: Terahertz Acoustic Vibration of Small Metal Nanoparticles", Nano Lett. **10**, 1853 (2010).

[87] J. S. Melinger, N. Laman, and D. Grischkowsky, "The underlying terahertz vibrational spectrum of explosives solids", Appl. Phys. Lett. **93**, (2008).

[88] M. Nagel, P. H. Bolivar, M. Brucherseifer, H. Kurz, A. Bosserhoff, and R. Buttner, "Integrated planar terahertz resonators for femtomolar sensitivity label-free detection of DNA hybridization", Appl. Optics **41**, 2074 (2002).

[89] C. K. Tiang, J. Cunningham, C. Wood, I. C. Hunter, and A. G. Davies, "Electromagnetic simulation of terahertz frequency range filters for genetic sensing", J Appl Phys **100**, (2006).

[90] M. J. Fitch, M. R. Leahy-Hoppa, E. W. Ott, and R. Osiander, "Molecular absorption cross-section and absolute absorptivity in the THz frequency range for the explosives TNT, RDX, HMX, and PETN", Chem Phys Lett **443**, 284 (2007).

[91] J. Kyoung, E. Y. Jang, M. D. Lima, H. R. Park, R. O. Robles, X. Lepro, Y. H. Kim, R. H. Baughman, and D. S. Kim, "A Reel-Wound Carbon Nanotube Polarizer for Terahertz Frequencies", Nano Lett. **11**, 4227 (2011).

[92] L. Ren, C. L. Pint, L. G. Booshenri, W. D. Rice, X. F. Wang, D. J.

Hilton, K. Takeya, I. Kawayama, M. Tonouchi, R. H. Hauge, and J. Kono, "Carbon Nanotube Terahertz Polarizer", Nano Lett. **9**, 2610 (2009).

[93] W. H. Zhang, L. N. Huang, C. Santschi, and O. J. F. Martin, "Trapping and Sensing 10 nm Metal Nanoparticles Using Plasmonic Dipole Antennas", Nano Lett. **10**, 1006 (2010).

[94] J. McPhillips, A. Murphy, M. P. Jonsson, W. R. Hendren, R. Atkinson, F. Hook, A. V. Zayats, and R. J. Pollard, "High-Performance Biosensing Using Arrays of Plasmonic Nanotubes", Acs Nano **4**, 2210 (2010).

[95] Craig F. Bohren and Donald R. Huffman, *Absorption and scattering of light by small particles*. (Wiley, New York, 1983).

[96] T. P. Bigioni, X. M. Lin, T. T. Nguyen, E. I. Corwin, T. A. Witten, and H. M. Jaeger, "Kinetically driven self assembly of highly ordered nanoparticle monolayers", Nat. Mater. **5**, 265 (2006).

[97] M. Osawa, "Dynamic processes in electrochemical reactions studied by surface-enhanced infrared absorption spectroscopy (SEIRAS)", B Chem Soc Jpn **70**, 2861 (1997).

요약(국문초록)

기존의 연구들을 통하여 광학 안테나는 국소 전자기장의 증폭 및 나노 입자 또는 생분자 검출과 관련하여 많은 관심을 받아왔다. 특히 광학 안테나를 이용하여 증폭된 강한 국소 전기장은 작은 입자로부터의 산란 및 비선형 방사(nonlinear emission) 현상을 증가시키며 결론적으로 빛의 회절 한계를 극복하면서 파장보다 훨씬 작은 입자들의 검출을 가능케 하였다. 이러한 기존 연구들을 바탕으로 본 논문에서는 광학 안테나의 개념을 테라헤르츠 주파수 대역에 적용시킨 테라헤르츠 나노 구멍 안테나에 대해 다룬다. 테라헤르츠 나노 구멍 안테나란 수백 마이크로미터 길이를 가지면서 수십 또는 수백 나노미터 너비를 지니는 직사각형 구멍 안테나를 말한다. 이 테라헤르츠 나노 안테나는 파장이 수백 마이크로미터에서 수 밀리미티에 이르는 테라헤르츠 전자기파의 나노미터 수준의 정밀한 제어를 가능하게 한다. 특히 본 논문에서는 테라헤르츠 주파수 대역에서 나노 구멍 안테나와 크기가 $\left(\frac{\lambda}{1{,}000}\right)^3$ 보다 작은 금속 나노 입자 사이의 강한 상호작용 현상에 대해 연구한다. 일반적으로 자유 공간에 있는 나노 입자는 그 단면(cross-section)이 매우 작아서 테라헤르츠 전자기파로는 검출이 불가능하다. 그러나 나노 입자를 나노 구멍 안테나 안에 놓았을 때, 우리는 둘 사이의 강한 상호작용 현상을 관찰할 수

있으며, 이러한 현상은 안테나 구멍 안에서의 다중 반사 효과로 인하여 나노 입자와 테라헤르츠 전자기파 사이의 실제 상호작용 빈도수가 크게 증가하기 때문에 나타난다. 이 뿐만 아니라, 이 논문에서는 나노 구멍 안테나에 대한 기본적인 특성에 대한 연구도 다루었는데, 나노 구멍 안테나 안에서의 강한 전기장 집속 현상과 수직 또는 수평 방향에 놓여 있는 두 인접한 나노 구멍 안테나 사이의 상호작용에 대한 연구를 수행하였다.

주요어: 테라헤르츠 시분할 분광, 테라헤르츠 나노 구멍 안테나, 나노 입자 검출, 테라헤르츠 광제어, 빛과 물질의 상호작용, 침투 깊이

학번: 2006-22905

List of publications

1. Terahertz pinch harmonics enabled by single nano rods

Hyeong-Ryeol Park, Young-Mi Bahk, Jong Ho Choe, Sanghoon Han, Seong Soo Choi, Kwang Jun Ahn, Namkyoo Park, Q-Han Park, and Dai-Sik Kim

Optics Express 19(24), 24775 (2011).

The Virtual Journal for Biomedical Optics 7(1) (2012)

Topic: Nanotechnology

2. Electrical control of terahertz nano antennas on VO2 thin film

Young-Gyun Jeong, Hannes Bernien, Ji-Soo Kyoung, Hyeong-Ryeol Park, Hyun‑Sun Kim, Jae-Wook Choi, Bong-Jun Kim, Hyun-Tak Kim, Kwang Jun Ahn, and Dai-Sik Kim

Optics Express 19, 21211 (2011).

3. Controlling terahertz radiation with nanoscale metal barriers embedded in nano slot antennas

Hyeong-Ryeol Park, Young-Mi Bahk, Kwang Jun Ahn, Q-Han Park, Dai-Sik Kim, Luis Martín-Moreno, Francisco J García-Vidal, and Jorge Bravo Abad

ACS NANO 5, 8340 (2011).

4. A reel-wound carbon nanotube polarizer for terahertz frequencies

Jisoo Kyoung, Eui Yun Jang, Marcio D. Lima, Hyeong-Ryeol Park, Raquel Ovalle Robles, Xavier Lepro, Yong Hyup Kim, Ray H. Baughman and Dai-Sik Kim

Nano Letters 11, 4227 (2011).

5. Nanopattern enabled terahertz all-optical switching on vanadium dioxide thin film

S. B. Choi, J. S. Kyoung, H. S. Kim, H. R. Park, Bong-Jun Kim, Y. H. Ahn, F. Rotermund, Hyun-Tak Kim, K. J. Ahn and D. S. Kim

Applied Physics Letters. 98, 071105 (2011).

6. Anomalous Band Formation in Arrays of Terahertz Nanoresonators

Y. M. Bahk, H. R. Park, K. J. Ahn, H. S. Kim, Y. H. Ahn, Dai-Sik Kim, J. Bravo-Abad, L. Martin-Moreno, and F. J. Garcia-Vidal

Physical Review Letters 106, 013902 (2011).

7. Far field detection of terahertz near field enhancement of sub-wavelength slits using Kirchhoff integral formalism

J. S. Kyoung, M. A. Seo, H. R. Park, K. J. Ahn and D. S. Kim

Optics communications 283, 4907 (2010).

8. Giant nonlinear response of terahertz nanoresonators on VO2 thin film

Jisoo Kyoung, Minah Seo, Hyeongryeol Park, Sukmo Koo, Hyun-sun Kim, Youngmi Park, Bong-Jun Kim, Kwangjun Ahn, Namkyoo Park, Hyun-Tak Kim, and Dai-Sik Kim

Optics Express 18, 16452 (2010).

9. Active Terahertz Nanoantennas Based on VO2 Phase Transition

Minah Seo, Jisoo Kyoung, Hyeongryeol Park, Sukmo Koo, Hyun-sun Kim,

Hannes Bernien, Bong Jun Kim, Jong Ho Choe, Yeong Hwan Ahn, Hyun-Tak Kim, Namkyoo Park, Q-Han Park, Kwangjun Ahn and Dai-sik Kim

Nano Letters 10, 2064 (2010).

10. Resonance behavior of single ultrathin slot antennas on finite dielectric substrates in terahertz regime

H. R. Park, S. M. Koo, O. K. Suwal, Y. M. Park, J. S. Kyoung, M. A. Seo, S. S. Choi, N. K. Park, D. S. Kim, and K. J. Ahn

Applied Physics Letters 96, 211109 (2010).

11. Terahertz Nano-Resonators: Giant Field Enhancement and Ultrabroadband Performance

H. R. Park, Y. M. Park, H. S. Kim, J. S. Kyoung, M. A. Seo, D. J. Park, Y. H. Ahn, K. J. Ahn, and D. S. Kim

Applied Physics Letters 96, 121106 (2010).

12. Focusing of terahertz waves onto micron-sized slits grown on ZnTe and GaP

M. A. Seo, H. R. Park, D. J. Park, Dai Sik Kim, A. J. L. Adam, and P. C. M. Planken

Journal of Korean Physical Society 55, 267 (2009).

13. Electromagnetic wave funneling through nano-gaps and nano-antennas

D. S. Kim, M. A. Seo, H. R. Park, J. S. Kyoung, J. W. Lee, O. K. Suwal, and S. S. Choi

(invited paper) Proc. SPIE 7214, 72140H (2009).

14. Terahertz field enhancement by a metallic nano slit operating beyond the skin-depth limit

M. A. Seo, H. R. Park, S. M. Koo, D. J. Park, J. H. Kang, O. K. Suwal, S. S. Choi, P. C. M. Planken, G. S. Park, N. K. Park, Q. H. Park, and D. S. Kim

Nature Photonics 3, 152 (2009).

Conferences

1. (Oral) Terahertz wave control enabled by nano objects embedded in slot antennas

Hyeong-Ryeol Park, Young-Mi Bahk, Kwang Jun Ahn, Q-Han Park2, Dai-Sik Kim, Luis Martín-Moreno, Francisco J. García-Vidal, and Jorge Bravo-Abad

CLEO 2012, 6-12 May, 2012, San Jose, USA

2. (Poster) Millimeter wave transmission control enabled by nanoscale objects embedded in nano slot antennas

H. R. Park, Y. M. Park, K. J. Ahn, Q-Han Park, D. S. Kim, L. Martín-Moreno, F. J. García-Vidal, and J. Bravo-Abad

Nanolight 2012, 11-17 March, 2012, Benasque, Spain.

3. (Oral) Strong coupling between terahertz nano slot antennas separated by sub-skin depth barriers.

Hyeong-Ryeol Park, Young-Mi Bahk, Jorge Bravo-Abad, Q-Han Park, Kwangjun Ahn, Francisco Garcia-Vidal, and Dai-Sik Kim

IRMMW-THz2011, 3-7 October, 2011, Hyatt Regency Houston, Houston, USA.

4. (Best student speech) Control of terahertz nanoresonator by a single metallic nanorod

H. R. Park, Y. M. Park, J. H. Choe, S. H. Han, O. K. Suwal, S. S. Choi, K. J. Ahn, N. K. Park, Q-Han Park, and D. S. Kim

Korean Physics Society 2010, 20-22 October, 2010, Pyeong Chang, Korea,

5. (Oral) Resonance frequency shifts of rectangular holes on finite dielectric substrates

H. R. Park, S. M. Koo, O. K. Suwal, Y. M. Park, J. S. Kyoung, M. A. Seo, S. S. Choi, N. K. Park, D. S. Kim, and K.J. Ahn

IRMMW-THz2010, 5-10 September, 2010, Angelicum, Rome, Italy,

6. (Poster) Pinch harmonic analogue of terahertz nanoresonator control using metal nano-rods

H. R. Park, S. M. Koo, Y. M. Park, M. A. Seo, O. K. Suwal, Q. Park, S. S. Choi, N. K. Park, K. J. Ahn, and D. S. Kim

IRMMW-THz2010, 5-10 September, 2010, Angelicum, Rome, Italy,

7. (Poster) Nearly-perfect ultrabroadband transmission of log-periodic terahertz nanoresonators

H. R. Park, Y. M. Park, H. S. Kim, J. S. Kyoung, M. A. Seo, D. J. Park, Y. H. Ahn, K. J. Ahn, and D. S. Kim

The Plasmonics Gordon Research Conference 2010, 13-18 June, 2010, Colby College, Waterville, ME, USA,

8. (Oral) Perfect Transmission of terahertz waves in periodic nanogap antennas

H. R. Park, Y. M. Park, H. S. Kim, J. S. Kyoung, M. A. Seo, K. J. Ahn, Y. H. Ahn, Q. H. Park and D. S. Kim

The 7th Asia-Pacific Conference on Near-field Optics (APNFO-7), 25-27 November, 2009, Jeju, Korea,

9. (Oral) Terahertz nanogap antenna for detection of nano-rods

H. R. Park, M. A. Seo, J. S Kyoung, J. H. Kang, Q-Han Park, O. K. Suwal, S. S. Choi, S. M. Koo, N. K. Park, D. S. Kim

IRMMW-THz2009, 21-25 September, 2009, Busan, Korea

10. (Oral) Terahertz nanogap antenna detection of nano-bridges and nano-rods

H. R. Park, M. A. Seo, J. S Kyoung, S. M. Koo, N. K. Park, O. K. Suwal, S. S. Choi, J. H. Kang, Q-Han Park, and D. S. Kim

2009 APS March Meeting , 16-20 March, 2009, Pittsburgh, USA

11. (Oral) Measurement and Calculation of Resonant Terahertz Transmission through Nano-Slits

H. R. Park, M. A. Seo, K. J. Ahn, O. K. Suwal, S. S. Choi, D. S. Kim

Korean Physics Society 2008, 22-24 October, 2008, Gwangju, Korea

Acknowledgement

감사의 글을 작성하기 위해 저의 지난 대학원 6년을 돌아보며 감사를 드려야 할 분의 명단을 작성해보니 어느덧 A4 용지 한 장이 훌쩍 넘어가고 있다는 사실을 깨달았습니다. 그 동안 졸업 심사며 논문이며, 저 하나만 생각하기에도 벅찬 나날들을 보내다가 오랜만에 한 발짝 뒤로 물러서서 다른 사람들의 고마움을 떠올릴 수 있는 그런 시간이 되었던 것 같습니다. 지금까지 제 인생이라는 경주 안에서 같이 뛰어주는 사람, 앞에서 끌어주는 사람, 뒤에서 밀어주는 사람, 그리고 밖에서 응원해주는 사람들, 이 모두가 함께 있었기에 저는 박사 졸업이라는 제 인생의 하나의 전환점에 올 수 있었습니다. 이 지면을 빌어서 그 분들 모두에게 짧게나마 감사의 인사를 올리며 이것이 제 고마움의 전부는 아니라는 것을 알아주셨으면 합니다.

첫 번째로 저의 박사과정 지도 교수님이신 김대식 교수님께 감사의 인사를 올립니다. 김 교수님께서는 지난 4년반동안 연구자로서 익혀야 할 많은 지식과 마인드, 실험 환경, 인적 네트워크까지 모두 주셨습니다. 그런 교수님의 지원과 기대에 반도 부응하지 못한 점을 죄송스럽게 생각하며 앞으로 더욱더 분발해야겠다는 생각을 다시금 하게 됩니다. 안광준 박사님 또한 같은 기간 동안 저에게는 연구자로서의 또 하나의 롤모델 이었으며 아낌없는 가르침과 격려를 주셨습니다.

처음에 연구실 들어왔을 때 FRET 실험을 가르쳐주시면서 연구자의 마인드를 알려주신 자일이형, 그 당시 같이 실험을 하며 열심히 가르쳐주던 정민이, 언제나 저의 어설픈 질문에 성심 성의껏

답변해주신 중욱이형, 비록 연구실에서 같이 생활한 시간은 짧았지만 스위스에서 친동생처럼 챙겨주셨던 광걸이형, 실험이든 연구든 언제나 제가 모르는 부분을 시원할 때까지 긁어주셨던 수봉이형과 두재형, 저에게 FIB를 가르쳐주신 여찬이형, 처음 연구실 들어갔을 때부터 따뜻하게 대해주신 진은누나, 제가 김대식 교수님 연구실에 들어올 수 있게 힘써주시고 대학원 기간 내내 정말 많은 도움을 주신 현우형, 테라헤르츠라는 분야를 시작하면서 가장 오랫동안 같이 일하고 기초부터 논문 쓰는 것까지 세세하게 가르쳐준 좋은 선배이자 파트너인 민아, 연구실에 있을 때 뿐만 아니라 KANC에 있을 때도 많은 도움과 지원을 해준 재성이, 학부생으로 같이 있으면서 서로 격려해주던 동호까지 연구실 선배님들의 자상하고 훌륭한 가르침 덕분에 오늘날의 제가 있게 된 것 같습니다.

민아 못지않게 오랫동안 테라헤르츠 분야에서 같이 일해온 지수, 방장으로서 교수님과 학생들 사이의 중계자 역할을 멋지게 잘 수행하면서 지금은 연구도 열심히 하는 영균이, 나의 대학원 후반기 연구에서 가장 열정적으로 도와주고 함께하였던 영미, 젠틀하고 똑똑한 규환이, 학부선배이자 연구실에 오셔서 많은 힘든 일을 멋지게 해결하신 석호형, 항상 나를 잘 따라주고 챙겨주는 완서, 밝은 표정으로 항상 파이팅 넘치는 지예, 논리적이고 주관이 또렷한 모습이 멋진 준연이, 성실하고 꾸준한 태희, 똑똑하면서 의젓하기도 한 덕형이, 착하고 부드러운 남자 광희, 박남규 교수님 연구실에 있을 때부터 나를 많이 도와주고 여기 와서도 열심히 잘하고 있는 상훈이, 이제 연구자로의 첫발을 내딛는 적극적인 모습이 좋아 보이는 지윤이까지 연구실 모든 후배들의 직간접적인 도움과

열정적인 모습들은 저에게 많은 자극과 힘이 되었습니다.

또한 센터연구원으로 재직하면서 아주대에서 샘플 제작에 고생 많이 하셨던 김현선씨와 최재욱씨, 장비 사용 및 여러 가지 도움을 주셨던 아주대 안영환 교수님과 박제구씨, 홍정택씨에게도 감사의 인사를 올립니다.

석사과정 동안 저의 또 한 분의 지도교수님이신 김재순 교수님의 열정적인 학구열과 학생 눈높이에 맞춘 수업들은 잊지 못할 것 같습니다. 석사 기간동안 같은 NIMO 연구실의 구성원이었던 플로리다에서 공부하고 있는 나락이형, 고대에서 postdoc하면서도 지금도 잊지 않고 잘 챙겨주는 문석이, 멋진 공군 장교님 기탁이형, LG에서 근무하는 관형이, KAIST에 가서도 잊지 않고 제 연구에 도움을 주시는 준엽이형과 석준이, 박사과정은 서로 다른 연구실에 속해있었지만 같은 연구실 멤버처럼 언제나 내 부탁을 흔쾌히 들어주는 형우까지 NIMO 연구실 모든 분들께도 감사의 인사를 올립니다.

제 연구에 훌륭한 협력자이자 아낌없는 조언을 주신 박남규 교수님, 박규환 교수님, 홍성철 교수님, 이기주 교수님, 구석모씨, 강지훈씨, 최종호씨, 상수형, 상화까지 모든 분들의 도움 덕택에 연구를 원활히 잘 수행하고 논문까지 잘 마무리할 수 있었습니다.

또한 비록 나라는 다르지만 만날 때마다 반갑게 맞아주시고 아낌없는 토론과 격려를 주시는 스페인(Spain)의 Francisco Garcia-Vidal 교수님과 Luis Martin-Moreno 교수님, Jorge Bravo-Abad 박사님, 나와 비슷하게 곧 졸업하는 Diego와 Paloma에게도 감사의 인사를 드립니다. (I would like to thank Prof. Francisco Garcia-Vidal, Prof. Luis

Martin-Moreno, Dr. Jorge Bravo-Abad, Diego, and Paloma for many stimulating discussions and our joint works.)

연구실에서 가장 궂은 일들을 맡아서 하시면서 저의 무지로 어렵게 꼬여버린 행정적인 일들을 멋지게 처리해주셨던 임소연씨, 이행도씨, 변수정씨에게도 감사의 인사를 올립니다.

그리고 저의 사랑하는 가족, 그 동안 묵묵히 지켜보시며 저의 대학원 생활 내내 물심양면 지원을 아낌없이 주시고 항상 저의 안식처가 되었던 부모님과 먼 미국에서 씩씩하게 잘 지내면서 오빠를 열심히 응원해주던 동생 지오, 찾아갈 때마다 반갑게 맞아주시고 저에게 역시 또 하나의 편한 안식처가 되어주셨던 장인어르신과 장모님, 나를 데리고 즐겁게 농구해주는 두 처남 경환이와 경준이, 생글생글 웃으면서 언제나 나에게 잘 대해주는 처제 경진이에게도 감사의 인사를 남깁니다.

마지막으로 저의 대학원 생활 시작할 때 만나서 박사 1학년 때 결혼을 하고 지금까지 함께해온 사랑하는 아내 경인, 대학원 생활 중 빼놓을 수 없는 가장 큰 축복이었으며 지금의 제 아내를 만나지 않았다면 과연 이렇게 잘 졸업까지 올 수 있었을지 의심을 해보게 됩니다. 그 동안 돈 한푼 벌어다 주지 못하고 남들 다 가는 휴가 한번 제대로 챙겨주지 못했음에도 불평하지 않고 항상 밝게 저를 응원해주는 당신께 정말 고맙고 사랑한다는 말을 전하고 싶습니다.